Extensions of the Standard Model scalar sector

Màster en Física Avançada
Especialitat de Física Teòrica

Ana Peñuelas Martínez*
Tutor: Antonio Pich Zardoya†

Curs 2015-2016

*apeumar@alumni.uv.es
†pich@ific.uv.es

Contents

Abstract

The existence of a Higgs-like boson with mass around 125 GeV is an undoubted fact supported by the last LHC data. The most simple model explaining such particle is the widely studied Standard Model. Despite this great predictive power some features of nature are not well explained only by the Standard Model. This motivates the study of extensions of the model as done here, where two enlargements of the scalar sector have been developed, analyzing the available data in these contexts by performing a χ^2 test. The 750 GeV diphoton excess recently observed in LHC and not explained by the Standard Model is also examined within these extensions.

1 Introduction

The Standard Model (SM) is the best and most simple theory describing strong, weak and electromagnetic interactions and giving us an extraordinary precision, which is increased everyday as particle accelerators and detectors are improved. Depending on their spin, particles of the SM are classified into *fermions* and *bosons*.

Fermions carry spin $\frac{1}{2}$ and in turn are divided into quarks and leptons, paired in three doublets corresponding to different generations, so that members of different generations carry the same quantum numbers.

On the other hand, gauge bosons carry spin 1 and act as mediator particles of interactions. These gauge bosons are the photon, γ, for the electromagnetic interaction, $W^{\pm}$ and Z for the weak force and the gluons, g, for the strong interaction. Given that the mass of the g and γ are zero as a result of gauge invariance, they are long-range interactions, unlike massive gauge bosons, whose interaction are short-range.

The last, but fundamental ingredient, needed in the SM is the Higgs boson, a particle carrying 0 spin and responsible of giving mass to weak bosons and fermions, in a process known as Spontaneous Symmetry Breaking (SSB) recently discovered at the LHC with a mass around 125 GeV. A general overview of the SM and SSB is given in sections 2 and 3.

Despite the great predictive power of the SM, some shortcomings seem to suggest the necessity of studying extensions of the model which would both include the content of the SM and the missing ingredients. Some of these open questions are CP violation, related to the matter-antimatter asymmetry or the content of dark matter in the Universe.

The Higgs mechanism of the SM is the most simple way of generating the masses of the particles, but different alternatives would both reproduce these as well as include some new and interesting ingredients.

Here, two of these models and their phenomenological implications will be studied. In Section 4 the most simple extension of the scalar sector of the SM, in which a real singlet is added, is presented, describing the SSB, the phenomenological features of the model and the study of its parameters using the last LHC data and performing a χ^2 minimization.

The other model studied in Section 5, is the so called Aligned Two-Higgs Doublet Model (A2HDM), in which a new doublet, with the same quantum numbers as the SM one is added. As for the Higgs singlet extension, the basic ingredients of the model are explained, now showing how the alignment in flavour space of the Yukawa couplings is imposed in order to avoid flavour-changing neutral currents (FCNC) at tree level. An analysis of the parameters from the last LHC data is performed in the different possible scenarios.

The last part of the work presented here corresponds to the study of the diphoton excess recently observed in the RUN2 of LHC, showing hints of a new resonance in the diphoton spectrum corresponding to an invariant mass around 750 GeV, which, if maintained once more data is acquired, would not be explained just by the SM.

2 The Standard Model

The SM is a gauge theory, based on the symmetry group $SU(3)_C \otimes SU(2)_L \otimes U(1)_Y$, which describes the strong, weak and electromagnetic interactions. After a process known as SSB, which will be explained in Section 3, this group is broken into $SU(3)_C \otimes U(1)_{QED}$ [1, 2, 3, 4].

2.1 Quantum Electrodynamics

The first piece needed to construct the SM is the Lagrangian describing a free fermion:

$$\mathcal{L}_0 = i\bar{\psi}(x)\gamma^\mu\partial_\mu\psi(x) - m\bar{\psi}(x)\psi(x)\,. \tag{1}$$

This Lagrangian is invariant under $U(1)$ transformations,

$$\psi(x) \xrightarrow{U(1)} \psi(x)' = e^{iQ\theta}\psi(x)\,, \tag{2}$$

$Q\theta$ is a real, arbitrary constant. However, it is very unnatural to look at *global* transformations of the fields. Instead we should consider *local* transformations, $\theta = \theta(x)$.

The gauge principle is the requirement that $U(1)$ holds locally. It is easy to check that imposing local transformations the Lagrangian is not invariant anymore due to the piece:

$$\partial_\mu\psi(x) \xrightarrow{U(1)} \partial_\mu\psi(x)' = e^{iQ\theta}\big(\,\partial_\mu + iQ\partial_\mu\theta(x)\,\big)\psi(x)\,. \tag{3}$$

To impose the gauge principle we need to add an extra piece to the Lagrangian, which is transformed in such a way that cancels the transformation of Eq. (3),

$$A_\mu(x) \xrightarrow{U(1)} A_\mu(x)' \equiv A_\mu(x) - \frac{1}{e}\partial_\mu\theta\,. \tag{4}$$

This new spin-1 field,[1] A_μ defines the covariant derivative:

$$D_\mu\psi(x) \equiv [\partial_\mu + ieQA_\mu(x)]\psi(x)\,, \tag{5}$$

which has the desired property of transforming like the field itself,

$$D_\mu\psi(x) \xrightarrow{U(1)} (D_\mu\psi(x))' = e^{iQ\theta}D_\mu\psi(x)\,. \tag{6}$$

And the new Lagrangian is invariant under local $U(1)$ transformations:

$$\mathcal{L} \equiv i\bar{\psi}(x)\gamma^\mu D_\mu\psi(x) - m\bar{\psi}(x)\psi(x) = \mathcal{L}_0 - eQA_\mu(x)\bar{\psi}(x)\gamma^\mu\psi(x)\,. \tag{7}$$

Note the new term in Eq. (7) describes the interaction between the fermionic field, $\psi(x)$, and the gauge field $A_\mu(x)$, which is the familiar Quantum Electrodynamics (QED) vertex. For $A_\mu(x)$ to be the true propagating field, the gauge invariant kinetic term has to be added:

$$\mathcal{L}_{\text{kin}} \equiv -\frac{1}{4}F_{\mu\nu}(x)F^{\mu\nu}(x)\,, \tag{8}$$

where $F_{\mu\nu} \equiv \partial_\mu A_\nu - \partial_\nu A_\mu$.

A mass term of the form $\mathcal{L}_m = \frac{1}{2}m^2 A_\mu A^\mu$ is forbidden, [2] because it would violate gauge invariance. This means we expect the photon to be massless, in agreement with our experimental results ($m_\gamma < 10^{-18}$ eV) [1].

Combining (7) and (8), the complete QED Lagrangian is:

$$\mathcal{L}_{QED} = \mathcal{L} + \mathcal{L}_{\text{kin}} = i\bar{\psi}(x)\gamma^\mu D_\mu\psi(x) - m\bar{\psi}(x)\psi(x) - \frac{1}{4}F_{\mu\nu}(x)F^{\mu\nu}(x)\,, \tag{9}$$

which gives rise to the well-known Maxwell equations:

$$\partial_\mu F^{\mu\nu} = eJ^\nu = eQ\bar{\psi}\gamma^\nu\psi\,. \tag{10}$$

[1] The field A_μ should be a spin-1 field since ∂_μ has a Lorentz index.

[2] Note: $F_{\mu\nu}(x) \xrightarrow{U(1)} F_{\mu\nu}(x)' = F_{\mu\nu}$, while $A_\mu(x)A^\mu(x) \xrightarrow{U(1)} A_\mu A^\mu - \frac{1}{e}(A_\mu\partial_\mu\theta + \partial_\mu\theta A^\mu) + \frac{1}{e^2}\partial_\mu\theta\partial_\mu\theta$.

2.2 Quantum Chromodynamics

Nowadays, it is an undeniable fact the existence of a deeper level of elementary constituents inside mesons and baryons: the *quarks*. Quantum Chromodynamics (QCD), is a non-Abelian gauge theory that describes the interaction through these elementary constituents (the quarks) and the gauge bosons of the theory, the *gluons* [5]. This theory is similar to QED, replacing the fermions by quarks and the photons by gluons, with the extra complication of being a non-Abelian theory.

In addition, to satisfy the Fermi-Dirac statistics the existence of a new quantum number, *colour*, is requiered in such a way that each quark may have $N_C = 3$ different colours ($q_\alpha, \alpha = 1, 2, 3$). Baryons and mesons are described by the colour-singlet combinations [2, 6]:

$$B = \frac{1}{\sqrt{6}}\epsilon^{\alpha\beta\gamma} |q_\alpha q_\beta q_\gamma\rangle \ , \qquad M = \frac{1}{\sqrt{3}}\delta^{\alpha\beta} |q_\alpha \bar{q}_\beta\rangle \ . \tag{11}$$

The fact that we do not observe colour states is related to the *confinement hypotesis* [7].

As we did for QED, let's start by writing the free Lagrangian of our theory

$$\mathcal{L}_0 = \sum_f \bar{q}_f (i\gamma^\mu \partial_\mu - m_f) q_f \ , \tag{12}$$

where q_f^α represents the field of a quark with colour α and flavour f and we have adopted a vector notation in colour space $q_f^T \equiv (q_f^1, q_f^2, q_f^3)$. In a similar way as before, the Lagrangian in Eq. (12) is invariant under a global $SU(3)_C$ transformation, [3]

$$q_f^\alpha \xrightarrow{SU(3)} (q_f^\alpha)' = U^\alpha_\beta q_f^\beta \ , \qquad UU^\dagger = U^\dagger U = 1 \, , \qquad \det U = 1 \, , \tag{13}$$

where U represents a $SU(3)_C$ matrix,

$$U = \exp\left\{ i\frac{\lambda_a}{2}\theta_a \right\} , \tag{14}$$

being $\frac{1}{2}\lambda^a, a = (1, ..8)$ the generators of the group in the fundamental representation and θ_a arbitrary parameters,[4]

As we did for QED we need to require our QCD Lagrangian to be invariant under *local* $SU(3)_C$ transformations, i.e $\theta_a = \theta_a(x)$. Imposing that, the quark fields are transformed as:

$$q_f^\alpha \xrightarrow{SU(3)_C} (q_f^\alpha)' = U^\alpha_\beta q_f^\beta = q_f^\alpha + i\left(\frac{\lambda_a}{2}\right)_{\alpha\beta} \delta\theta_a q_f^\beta \, . \tag{15}$$

And for the Lagrangian we have the following transformation:

$$\mathcal{L}_0 \xrightarrow{SU(3)_C} \mathcal{L}_0' = \sum_f \bar{q}_f \Big(i\gamma^\mu \frac{i\lambda_a}{2}\partial_\mu \theta_a + i\gamma^\mu \partial_\mu - m_f \Big) q_f \ , \tag{16}$$

which is not invariant under $SU(3)_C$. To make it invariant the usual derivatives need to be replaced by covariant derivatives,

$$D^\mu q_f = \Big[\partial_\mu + ig_s \frac{\lambda_a}{2} G_a^\mu(x) \Big] q_f \equiv \Big[\partial_\mu + ig_s G^\mu(x) \Big] q_f \ , \tag{17}$$

where in the last step we just have introduced a more compact notation.[5]

[3] The fact that the symmetry is described by the group $SU(N_C)$ is related to the quantum number colour. In QED our Lagrangian was invariant under charge Q, now it is invariant under transformations in colour space.

[4] These are traceless matrices $Tr(\lambda_a) = 0$ and satisfy the commutation relations $[\frac{\lambda_a}{2}, \frac{\lambda_b}{2}] = if^{abc}\frac{\lambda_c}{2}$, being f^{abc} $SU(3)_C$ structure constants.

[5] $[G^\mu]_{\alpha\beta} \equiv \Big((\frac{\lambda_a}{2})_{\alpha\beta} G_a^\mu(x) \Big)$.

As a result, there will be eight new gauge bosons, [6] the gluons, G_a^μ, which apart from the usual Lorentz index, μ carry colour (a).

The transformation properties of D_μ are fixed by the requirement of $D_\mu q_f$ to transform as the colour-vector q_f:

$$D^\mu \xrightarrow{SU(3)_C} (D^\mu)' = U D^\mu U^\dagger \,, \qquad G^\mu \xrightarrow{SU(3)_C} U G^\mu U^\dagger + \frac{i}{g_s}(\partial^\mu U)U^\dagger \,. \tag{18}$$

The infinitesimal transformations of the quark fields are given by Eq. (15) and for the gluon fields:

$$G_a^\mu \xrightarrow{SU(3)_C} (G_a^\mu)' = G_a^\mu - \frac{1}{g_s}\partial^\mu(\delta\theta_a) - f^{abc}\delta\theta_b G_c^\mu \,. \tag{19}$$

As we did in QED, the next step is to build a gauge-invariant kinetic term. To do that the corresponding field strengths need to be introduced:

$$\begin{gathered} G^{\mu\nu}(x) \equiv -\frac{i}{g_s}[D_\mu, D_\nu] = \partial^\mu G^\nu - \partial^\nu G^\mu + i g_s [G^\mu, G^\nu] \equiv \frac{\lambda_a}{2} G_a^{\mu\nu}(x) \,, \\ G_a^{\mu\nu}(x) = \partial^\mu G_a^\nu - \partial^\nu G_a^\mu - g_s f^{abc} G_b^\mu G_c^\nu \,, \end{gathered} \tag{20}$$

with

$$G^{\mu\nu} \xrightarrow{SU(3)_C} (G^{\mu\nu})' = U G^{\mu\nu} U^\dagger \,. \tag{21}$$

Since gauge invariance forbids adding a mass term for the gluon fields, they will remain as massless spin-1 particles. Now we are able to write the full QCD Lagrangian,

$$\mathcal{L}_{QCD} = -\frac{1}{4} G_a^{\mu\nu} G^a_{\mu\nu} + \sum_f \bar{q}_f (i\gamma^\mu D_\mu - m_f) q_f \,. \tag{22}$$

And developing the Lagrangian of Eq. (22) we can look at the different contributions:

$$\begin{gathered} \mathcal{L}_{QCD} = \underbrace{-\frac{1}{4}(\partial^\mu G_a^\nu - \partial^\nu G_a^\mu)(\partial_\mu G^a_\nu - \partial_\nu G^a_\mu) + \sum_f \bar{q}_f^\alpha (i\gamma^\mu \partial_\mu - m_f) q_f^\alpha}_{\text{quadratic kinetic terms}} \\ \underbrace{-g_s G_a^\mu \sum_f \bar{q}_f^\alpha \gamma^\mu \left(\frac{\lambda_a}{2}\right)_{\alpha\beta} q_f^\beta}_{\text{colour interaction between quarks and gluons}} \\ \underbrace{+\frac{g_s}{2} f^{abc} (\partial^\mu G_a^\nu - \partial^\nu G_a^\mu) G^b_\mu G^c_\nu - \frac{g_s^2}{4} f^{abc} f_{ade} G_b^\mu G_c^\nu G^d_\mu G^e_\nu}_{\text{cubic and quartic gluon self interaction}} \,. \end{gathered} \tag{23}$$

Looking at the form of the Lagrangian we can identify the quadratic term, that will give us the propagators, the interaction between gluons and quarks and finally the gluon self interactions, which are due to the non-Abelian character of the theory.

2.3 Electroweak Unification

The model describing weak interactions is the Electroweak model, based on the symmetry group $G \equiv SU(2)_L \otimes U(1)_Y$. Now, the complexity is increased, since we need to express the different behaviour of the left and right-handed fields, and the massive bosons $W^\pm$ and Z that were not present in the case of QED and QCD have to be included.

[6] $8 = N_c^2 - 1 = 9 - 1$.

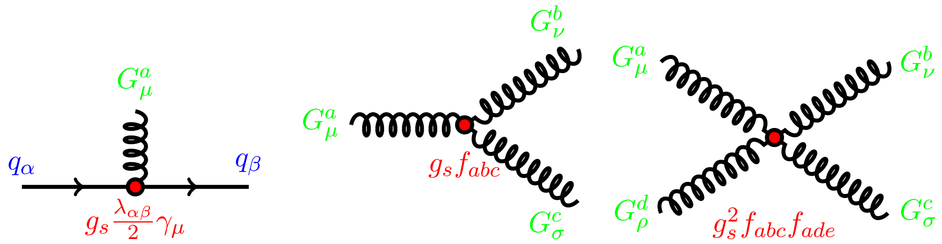

Figure 1: Interaction vertices of the QCD Lagrangian.

In the SM there are three families of quarks and fermions, which can be expressed as:

$$\begin{bmatrix} \nu_e & u \\ e^- & d' \end{bmatrix} , \qquad \begin{bmatrix} \nu_\mu & c \\ \mu^- & s' \end{bmatrix} , \qquad \begin{bmatrix} \nu_\tau & t \\ \tau^- & b' \end{bmatrix} , \tag{24}$$

where each matrix represents the lepton sector (left column) and the quark sector (right column) of each family. Taking any of these families for quarks we have:

$$\psi_1(x) = \begin{bmatrix} u \\ d \end{bmatrix}_L , \qquad \psi_2(x) = u_R \, , \qquad \psi_3(x) = d_R \, . \tag{25}$$

And for leptons:

$$\psi_1(x) = \begin{bmatrix} \nu_3 \\ e^- \end{bmatrix}_L , \qquad \psi_2(x) = \nu_{eR} \, , \qquad \psi_3(x) = e^-_R \, . \tag{26}$$

As we did for QED and QCD we start by considering the free Lagrangian [7]

$$\mathcal{L}_0 = i\bar{u}(x)\gamma^\mu \partial_\mu u(x) + i\bar{d}(x)\gamma^\mu \partial_\mu d(x) = \sum_{j=1}^{3} i\bar{\psi}_j(x)\gamma^\mu \partial_\mu \psi_j(x) \, , \tag{27}$$

with

$$u(x) = \begin{bmatrix} u_R \\ u_L \end{bmatrix} , \qquad d(x) = \begin{bmatrix} d_R \\ d_L \end{bmatrix} . \tag{28}$$

The Lagrangian, $\mathcal{L}_0$, is invariant under a global transformation of the fields under the group G,

$$\begin{aligned} \psi_1(x) &\xrightarrow{G} \psi_1(x)' \equiv \exp\{iy_1\beta\} U_L \psi_1(x) \, , \\ \psi_2(x) &\xrightarrow{G} \psi_2(x)' \equiv \exp\{iy_2\beta\} \psi_2(x) \, , \\ \psi_3(x) &\xrightarrow{G} \psi_3(x)' \equiv \exp\{iy_3\beta\} \psi_3(x) \, , \end{aligned} \tag{29}$$

where the part of (29) proportional to the exponential is the transformation under the group $U(1)_Y$, with the parameters y_i, the hypercharges, and the part corresponding to the $SU(2)_L$ group is related to the non-abelian matrix transformation U_L, (σ_i are the Pauli matrices),

$$U_L \equiv \exp\left\{ i\frac{\sigma_i}{2}\alpha^i \right\} , \tag{30}$$

and consequently it only acts on the left-handed components, i.e. it only acts on $\psi_1(x)$.

By requiring the Lagrangian to be also invariant under local transformations, $\alpha^i = \alpha^i(x)$ and $\beta^i = \beta^i(x)$, we are forded to include the following covariant derivatives:

[7]We have not included a mass term in (27) because it would have mixed the left and right-handed fields.

$$D_\mu\psi_1(x) \equiv [\partial_\mu + ig\widetilde{W}_\mu(x) + ig'y_1 B_\mu(x)]\psi_1(x)\,, \tag{31}$$
$$D_\mu\psi_2(x) \equiv [\partial_\mu + ig'y_2 B_\mu(x)]\psi_2(x)\,,$$
$$D_\mu\psi_3(x) \equiv [\partial_\mu + ig'y_3 B_\mu(x)]\psi_3(x)\,,$$

where

$$\widetilde{W}_\mu(x) \equiv \frac{\sigma_i}{2} W^i_\mu(x)\,. \tag{32}$$

The requisite that $D_\mu\psi_j(x)$ is transformed as $\psi_j(x)$ fixes the transformation of the gauge fields:

$$B_\mu(x) \xrightarrow{G} B'_\mu(x) \equiv B_\mu(x) - \frac{1}{g'}\partial_\mu\beta(x)\,, \tag{33}$$
$$\widetilde{W}_\mu(x) \xrightarrow{G} \widetilde{W}'_\mu(x) \equiv U_L\widetilde{W}_\mu(x)U_L^\dagger + \frac{i}{g}\partial_\mu U_L(x)U_L(x)^\dagger\,.$$

These transformations remind us of the ones of QED (B_μ) and QCD ($\widetilde{W}_\mu$).

To continue with our analysis we have to add all the possible gauge-invariant kinetic terms for the gauge terms. Introducing the field strengths:

$$B_{\mu\nu} \equiv \partial_\mu B_\nu - \partial_\nu B_\mu\,, \tag{34}$$
$$\widetilde{W}_{\mu\nu} \equiv -\frac{i}{g}\left[\left(\partial_\mu + ig\widetilde{W}_\mu\right)\left(\partial_\nu + ig\widetilde{W}_\nu\right)\right] = \partial_\mu\widetilde{W}_\nu - \partial_\nu\widetilde{W}_\mu + ig[\widetilde{W}_\mu,\widetilde{W}_\nu]\,,$$
$$\widetilde{W}_{\mu\nu} \equiv \frac{\sigma_i}{2}W^i_{\mu\nu}\,, \qquad W^i_{\mu\nu} = \partial_\mu W^i_\nu - \partial_\nu W^i_\mu - g\epsilon^{ijk}W^j_\mu W^k_\nu\,.$$

Under a G transformation:

$$B_{\mu\nu} \xrightarrow{G} B_{\mu\nu}\,, \qquad \widetilde{W}_{\mu\nu} \xrightarrow{G} U_L\widetilde{W}_{\mu\nu}U_L^\dagger\,. \tag{35}$$

And the kinetic Lagrangian, with the pertinent normalization is

$$\mathcal{L}_{\text{kin}} = -\frac{1}{4}B_{\mu\nu}B^{\mu\nu} - \frac{1}{2}\,\text{Tr}\left[\widetilde{W}_{\mu\nu}\widetilde{W}^{\mu\nu}\right] = -\frac{1}{4}B_{\mu\nu}B^{\mu\nu} - \frac{1}{4}W^i_{\mu\nu}W_i^{\mu\nu}\,. \tag{36}$$

Since the field strengths of Eq. (36) contain quadratic pieces, $\mathcal{L}_{\text{kin}}$ will contain cubic and quartic self-interactions between the gauge bosons. In addition, we can note that we are not allowed to add a mass term neither for bosons, since it will break gauge symmetry, nor for fermions, because it will imply an interaction between left and right-handed fields, with different transformation properties.

2.3.1 Charged-current interactions

In this section we will briefly introduce the part of the Lagrangian that gives rise to the interaction between fermions and charged bosons ($W^\pm$),

$$\mathcal{L} = \sum_{j=1}^{3} i\overline{\psi}_j(x)\gamma^\mu\partial_\mu\psi_j(x) - g\overline{\psi}_1(x)\gamma^\mu\widetilde{W}_\mu\psi_1(x) - g'B_\mu\sum_{j=1}^{3}\overline{\psi}_j(x)\gamma^\mu\psi_j(x)\,. \tag{37}$$

The first piece is the kinetic term for the fermions, while the second and the third terms will give us the interaction between the fermions and the gauge bosons. To obtain the charged-current (CC) interactions we should note:

$$\widetilde{W}_\mu = \frac{\sigma^i}{2}W^i_\mu = \frac{1}{2}\begin{bmatrix} W^3_\mu & \sqrt{2}W^\dagger_\mu \\ \sqrt{2}W_\mu & -W^3_\mu \end{bmatrix}\,, \tag{38}$$

where the CC contribution will be due to the term $W^\dagger_\mu \equiv (W^1_\mu - iW^2_\mu)/\sqrt{2}$, and W^3_μ will contribute to the neutral-current (NC), as we will see in the next section. The Lagrangian of the CC, for any family of quarks and leptons is:

$$\mathcal{L}_{CC} = -\frac{g}{2\sqrt{2}}\left\{W^\dagger_\mu[\bar{u}\gamma^\mu(1-\gamma_5)d + \nu_l\gamma^\mu(1-\gamma_5)l^-] + \text{h.c.}\right\}\,. \tag{39}$$

and it will give rise to the vertices of Fig. 2.

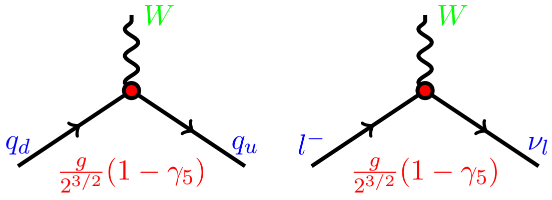

Figure 2: Charged-current interaction vertices.

2.3.2 Neutral-current interactions

As we can see from Eq. (37), our Lagrangian also contains NC interactions, that will come both from the second term (interactions with W_μ^3) and third term (interactions with B_μ) of Eq. (37).

At first, we could think of identifying these fields with the Z boson and the photon, γ. But given that the photon has the same interaction with both fermion chiralities, the field B_μ cannot be equal to the electromagnetic field.[8] Instead, it seems natural to work with an arbitrary combination of the fields:

$$\begin{bmatrix} W_\mu^3 \\ B_\mu \end{bmatrix} = \begin{bmatrix} \cos\theta_\mathrm{w} & \sin\theta_\mathrm{w} \\ -\sin\theta_\mathrm{w} & \cos\theta_\mathrm{w} \end{bmatrix} \begin{bmatrix} Z_\mu \\ A_\mu \end{bmatrix} . \tag{40}$$

And, expressing the NC Lagrangian in terms of these fields we have

$$\mathcal{L}_{NC} = -\sum_j \bar{\psi}_j(x)\gamma^\mu \left\{ A_\mu \left[g\frac{\sigma_3}{2}\sin\theta_\mathrm{w} + g' y_j \cos\theta_\mathrm{w} \right] + Z_\mu \left[g\frac{\sigma_3}{2}\cos\theta_\mathrm{w} - g' y_j \sin\theta_\mathrm{w} \right] \right\} \psi_j \, . \tag{41}$$

To recover QED from the A_μ piece we impose:

$$g\sin\theta_\mathrm{w} = g'\cos\theta_\mathrm{w} = e \, , \qquad Y = Q - T_3 \, , \tag{42}$$

where the electromagnetic charge operator, Q, is expressed as:

$$Q_1 = \begin{bmatrix} Q_{u/\nu} & 0 \\ 0 & Q_{d/e} \end{bmatrix} , \qquad Q_2 = Q_{u/\nu} \, , \qquad Q_3 = Q_{d/e} \, , \tag{43}$$

and $T_3 \equiv \frac{\sigma_3}{2}$.

The form of the hypercharge, Y, comes from the fact that it should be a linear combination of Q and T_3 and the requirement that it commutes with the involved operators, and fixes the hypercharge of the fermions:

$$\begin{array}{lll} \text{Quarks: } y_1 = Q_u - \frac{1}{2} = Q_d + \frac{1}{2} = \frac{1}{6}, & y_2 = Q_u = \frac{2}{3}, & y_3 = Q_d = -\frac{1}{3}. \\ \text{Leptons: } y_1 = Q_\nu - \frac{1}{2} = Q_e + \frac{1}{2} = -\frac{1}{2}, & y_2 = Q_\nu = 0, & y_3 = Q_e = -1. \end{array}$$

The NC Lagrangian reads:

$$\mathcal{L}_{NC} = \mathcal{L}_{QED} + \mathcal{L}_{NC}^Z \, , \tag{44}$$

where

$$\mathcal{L}_{QED} = -eA_\mu \sum_j \bar{\psi}_j \gamma^\mu Q_j \psi_j \equiv -eA_\mu J_\mathrm{em}^\mu \, , \tag{45}$$

for the QED part and

$$\mathcal{L}_{NC}^Z = -\frac{e}{2\sin\theta_\mathrm{w}\cos\theta_\mathrm{w}} J_Z^\mu Z_\mu \, , \tag{46}$$

$$J_Z^\mu \equiv \sum_j \bar{\psi}_j \gamma^\mu (\sigma_3 - 2\sin^2\theta_\mathrm{w} Q_j)\psi_j = J_3^\mu - 2\sin^2\theta_\mathrm{w} J_\mathrm{em}^\mu \, ,$$

[8] That would require $y_1 = y_2 = y_3$ and $g' y_j = eQ_j$, which cannot be simultaneously true.

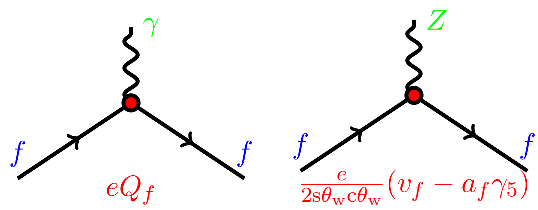

Figure 3: Neutral-current interaction vertices with $s\theta_w \equiv \sin\theta_w$ and $c\theta_w \equiv \cos\theta_w$.

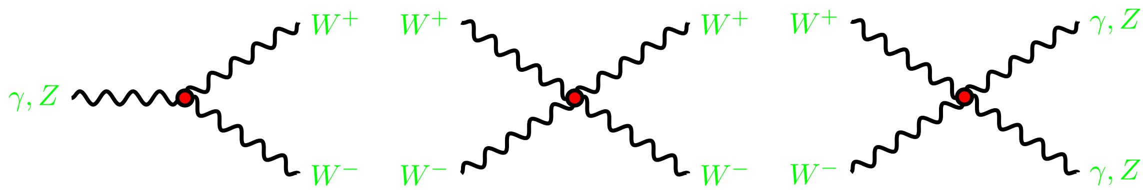

Figure 4: Self-interaction vertices of the gauge bosons.

or in terms of the fermion fields

$$\mathcal{L}_{NC}^{Z} = -\frac{2}{2\sin\theta_w\cos\theta_w} Z_\mu \sum_f \bar{f}\gamma^\mu(v_f - a_f\gamma_5)f\,, \tag{47}$$

where $a_f = T_3^f$ and $v_f = T_3^f(1 - 4|Q_f|\sin^2\theta_w)$.

2.3.3 Gauge self-interactions

As we can see from the term in (36), we will have cubic and quartic self-interactions between the gauge bosons (Fig. 3):

$$\begin{aligned}\mathcal{L}_3 = ie\cot\theta_w &\left\{(\partial^\mu W^\nu - \partial^\nu W^\mu)W_\mu^\dagger Z_\nu - (\partial^\mu W^{\nu\dagger} - \partial^\nu W^{\mu\dagger})W_\mu Z_\nu + W_\mu W_\nu^\dagger(\partial^\mu Z^\nu - \partial^\nu Z^\mu)\right\} \\ &+ie\left\{(\partial^\mu W^\nu - \partial^\nu W^\mu)W_\mu^\dagger A_\nu - (\partial^\mu W^{\nu\dagger} - \partial^\nu W^{\mu\dagger})W_\mu A_\nu + W_\mu W_\nu^\dagger(\partial^\mu A^\nu - \partial^\nu A^\mu)\right\}\,,\end{aligned} \tag{48}$$

$$\begin{aligned}\mathcal{L}_4 = -\frac{e^2}{2\sin^2\theta_w}&\left\{\left(W_\mu^\dagger W^\mu\right)^2 - W_\mu^\dagger W^{\mu\dagger} W_\nu W^\nu\right\} - e^2\cot^2\theta_w\left\{W_\mu^\dagger W^\mu Z_\nu Z^\nu - W_\mu^\dagger Z^\mu W_\nu Z^\nu\right\} \\ &-e^2\cot\theta_w\left\{2W_\mu^\dagger W^\mu Z_\nu A^\nu - W_\mu^\dagger Z^\mu W_\nu A^\nu - W_\mu^\dagger A^\mu W_\nu Z^\nu\right\} \\ &-e^2\left\{W_\mu^\dagger W^\mu A_\nu A^\nu - W_\mu^\dagger A^\mu W_\nu A^\nu\right\}\,.\end{aligned} \tag{49}$$

3 Spontaneous Symmetry Breaking

In our description of Electroweak Unification gauge bosons are massless particles, while our experience tells us that $W^\pm$ and Z should be massive bosons.

To generate masses, we need to break gauge symmetry. However, this has to be done carefully, since we also need a fully symmetric Lagrangian in order to preserve renormalizability.

This can be done through a process known as SSB [8, 9, 10, 11, 12], in which we have a Lagrangian invariant under a group of transformations that has a degenerate set of states with minimal energy. The fact of selecting one of these states as the ground state will spontaneously break the symmetry, leading to the appearance of new spin-0 massless particles, as we will see in the next section.

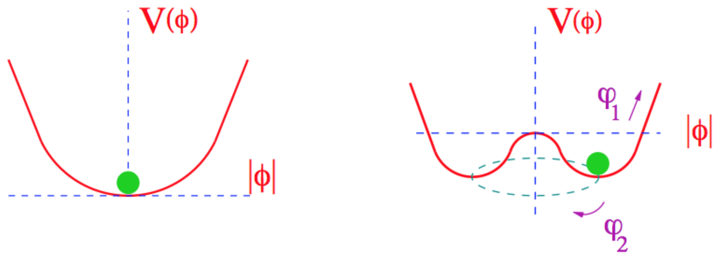

Figure 5: Potential for the two different values of μ^2. In the left potential we can see there is only one minimum, while in the right there is an infinite number of degenerate states.

3.1 Goldstone Theorem

In order to illustrate the main idea of the Goldstone theorem, let's consider a complex scalar field, $\phi(x)$, and the following Lagrangian:

$$\mathcal{L} = \partial_\mu \phi(x)^\dagger \partial^\mu \phi(x) - V(\phi)\,, \qquad V(\phi) = \mu^2 \phi^\dagger \phi + h(\phi^\dagger \phi)^2\,. \tag{50}$$

where $\mathcal{L}$ is invariant under a global phase transformation,

$$\phi(x) \to \phi(x)' = e^{i\theta}\phi(x)\,. \tag{51}$$

If we focus in the form of the potential, we can note h should be positive, for the potential to be bounded from below. For the parameter μ^2 we have two different possibilities, as it can be seen in Fig. 5:

- **1.** $\mu^2 > 0$**:** The only minimum of $V(\phi)$ is $\phi = 0$, so there is not a degenerate set of states.
- **2.** $\mu^2 < 0$**:** There is an infinity set of minima satisfying the condition $|\phi_0(x)| = \sqrt{\frac{-\mu^2}{2h}} = \frac{v}{\sqrt{2}}$. Now we are in the case mentioned before in which we have a degenerate set of states of minimum energy.

We will focus in case **2**, in which there is a degenerate set of minima. If we choose one of these minima, for instance, $\phi_0(x) = \frac{v}{\sqrt{2}}$, the symmetry gets spontaneously broken. To continue, let's parametrize excitations over the ground state as:

$$\phi(x) = \frac{1}{\sqrt{2}}\Big(v + \varphi_1(x) + i\varphi_2(x)\Big)\,, \tag{52}$$

where φ_1 and φ_2 are real fields.

Parameterizing the potential in this way we get:

$$V(\phi) = V(\phi_0) - \mu^2\varphi_1^2 + hv\varphi_1(\varphi_1^2 + \varphi_2^2) + \frac{h}{4}(\varphi_1^2 + \varphi_2^2)^2\,. \tag{53}$$

From here we can see φ_1 describes a state with mass $m^2_{\varphi_1} = -2\mu^2$, while φ_2 is massless and describes excitations around the flat direction of the potential, where the energy is the same (ground state). This is a general result, known as **Goldstone Theorem**: If a Lagrangian is invariant under a continuous symmetry group G, but the vacuum is only invariant under a subgroup $H \subset G$, then there must exist as many massless spin-0 particles (Nambu-Goldstone bosons) as broken generators (i.e. generators of G which don't belong to H).

3.2 Higgs Boson

In this section we will see how, as a result of the Goldstone Theorem, the $W^{\pm}$ and Z bosons acquire mass, while A^{μ} remains massless.

To do that let's consider a $SU(2)_L$ doublet of complex scalar fields

$$\phi(x) = \begin{bmatrix} \phi^{(+)}(x) \\ \phi^{(0)}(x) \end{bmatrix} , \tag{54}$$

and a gauged scalar Lagrangian invariant under $SU(2)_L \otimes U(1)_Y$ transformations

$$\begin{aligned} \mathcal{L}_s &= (D_\mu \phi)^\dagger D^\mu \phi - \mu^2 \phi^\dagger \phi - h(\phi^\dagger \phi)^2 , \qquad (h > 0, \mu^2 < 0) , \\ D^\mu \phi &= \left\{ \partial^\mu + ig\widetilde{W}^\mu + ig' y_\phi B^\mu \right\} \phi , \qquad y_\phi = Q_\phi - T_3 = \frac{1}{2} . \end{aligned} \tag{55}$$

The value of the hypercharge is fixed by the requirement of having the correct coupling between $\phi(x)$ and $A^\mu(x)$ ($\phi^{(0)}$ not coupled to the photon and $\phi^{(+)}$ the right charge).

Looking for the minimum of the potential,

$$\frac{\partial V}{\partial |\phi|} = 0 \rightarrow |\phi| = 0, |\phi| = \sqrt{\frac{-\mu^2}{2h}} . \tag{56}$$

Since $\phi^{(+)}$ is charged its vev would be 0:

$$\langle 0 | [\mathcal{Q}, \phi^{(+)}(x)] | 0 \rangle = Q \langle 0 | \phi^{(+)}(x) | 0 \rangle = \langle 0 | \mathcal{Q}, \phi^{(+)}(x) | 0 \rangle - \langle 0 | \phi^{(+)}(x) \mathcal{Q} | 0 \rangle = 0 \rightarrow \langle 0 | \phi^{(+)}(x) | 0 \rangle = 0 . \tag{57}$$

And this does not happen for $\phi^{(0)}$ since it is neutral ($Q = 0$). So, only the neutral component of the doublet will acquire a vacuum expectation value,

$$| \langle 0 | \phi | 0 \rangle | = \begin{bmatrix} 0 \\ | \langle 0 | \phi^{(0)} | 0 \rangle | \end{bmatrix} = \begin{bmatrix} 0 \\ \sqrt{\frac{-\mu^2}{2h}} \end{bmatrix} . \tag{58}$$

There is an infinite set of states, differing by a phase, that satisfy Eq. (58). Once we choose a particular ground state, for example

$$\langle 0 | \phi^{(0)} | 0 \rangle = \sqrt{\frac{-\mu^2}{2h}} \equiv \frac{v}{\sqrt{2}} , \tag{59}$$

the $SU(2)_L \otimes U(1)_Y$ symmetry gets broken to the electromagnetic group $U(1)_Q$, which remains a symmetry of the vacuum.

As before, we will parametrize our doublet considering excitations over the physical vacuum

$$\phi(x) = \exp\left\{ i \frac{\sigma_i}{2} \theta^i(x) \right\} \frac{1}{\sqrt{2}} \begin{bmatrix} 0 \\ \frac{v + H(x)}{\sqrt{2}} \end{bmatrix} . \tag{60}$$

Before moving on, and remembering the Goldstone Theorem of Section 3.1, let's look at the generators of the groups we are working with. The four generators of $G = SU(2)_L \otimes U(1)_Y$ are $\frac{\sigma_i}{2}$ (three generators for $SU(2)$) and Y (one generator for $U(1)$). The generator of the group $U(1)_Q$ into which G gets broken is Q. We say a generator is broken if:

$$T_a \phi_0 \neq 0 , \tag{61}$$

being $\phi_0 = \frac{1}{\sqrt{2}} \begin{bmatrix} 0 \\ v \end{bmatrix}$ the vev of the doublet. To identify the broken and unbroken generators:

$$\begin{aligned}
T_1\phi_0 &= \frac{\sigma_1}{2}\phi_0 = \frac{1}{2\sqrt{2}}\begin{bmatrix} v \\ 0 \end{bmatrix} \neq 0\,, \\
T_2\phi_0 &= \frac{\sigma_2}{2}\phi_0 = -\frac{i}{2\sqrt{2}}\begin{bmatrix} v \\ 0 \end{bmatrix} \neq 0\,, \\
T_3\phi_0 &= \frac{\sigma_3}{2}\phi_0 = \frac{1}{2\sqrt{2}}\begin{bmatrix} 0 \\ -v \end{bmatrix} \neq 0\,, \\
Y\phi_0 &= \frac{1}{2\sqrt{2}}\begin{bmatrix} 0 \\ v \end{bmatrix} \neq 0\,, \\
Q\phi_0 &= (Y+T_3)\phi_0 = \begin{bmatrix} 0 \\ 0 \end{bmatrix} = 0\,.
\end{aligned} \tag{62}$$

With that we have checked there are three broken generators. We can also note, that after the SSB there are four degrees of freedom (three $\theta^i(x)$ and $H(x)$). Since we have local $SU(2)_L$ invariance we can choose a particular gauge for which $\theta^i(x) = 0$, [9]

$$\phi(x) = \frac{1}{\sqrt{2}}\begin{bmatrix} 0 \\ v + H(x) \end{bmatrix}\,. \tag{63}$$

With this gauge, the kinetic term of the Lagrangian is:

$$\mathcal{L}_{\text{kin}} = \frac{1}{2}\left\{(\partial_\mu H)(\partial^\mu H) + (v+H)^2\Big(\frac{g^2}{4}W_\mu^\dagger W_\mu + \frac{g^2}{8\cos^2\theta_{\text{w}}}Z_\mu Z^\mu\Big)\right\}\,. \tag{64}$$

The vacuum expectation value of the neutral scalar doublet has generated a mass term for the gauge bosons $W^\pm$ and Z. These mass terms are:

$$\begin{aligned}
&\frac{v^2g^2}{4} = M_W^2 \to M_W = \frac{vg}{2}\,, \\
&\frac{v^2g^2}{8\cos^2\theta_{\text{w}}} = \frac{1}{2}M_Z^2 \to M_Z = \frac{vg}{2\cos\theta_{\text{w}}}\,, \\
&0 = \frac{1}{2}M_A^2 \to M_A = 0\,.
\end{aligned} \tag{65}$$

At this point it can be seen how the SSB has generated the masses of the gauge bosons. Furthermore, since Q is an unbroken generator, the photon remain massless, and there is a new scalar particle: the Higgs boson.

To finish with this Section let's count the degrees of freedom. **Before** the SSB we had 10 degrees of freedom (d.o.f): three massless boson fields $W^\pm$ and Z ($3\times 2 = 6$ d.o.f), and four real scalars (4 d.o.f). **After** the SSB we have 10 d.o.f: three massive bosons ($3\times 3 = 9$ d.o.f) and the Higgs boson (1 d.o.f).

The Lagrangian that describes this new particle, the Higgs boson is:

$$\mathcal{L}_S = \frac{1}{4}hv^4 + \mathcal{L}_H + \mathcal{L}_{HG^2}\,, \tag{66}$$

where

$$\begin{aligned}
\mathcal{L}_H &= \frac{1}{2}\partial_\mu H\partial^\mu H - \frac{1}{2}M_H^2H^2 - \frac{M_H^2}{2v}H^3 - \frac{M_H^2}{8v^2}H^4\,, \\
\mathcal{L}_{HG^2} &= M_W^2 W_\mu^\dagger W^\mu\left\{1 + \frac{2}{v}H + \frac{H^2}{v^2}\right\} + \frac{1}{2}M_Z^2 Z_\mu Z^\mu\left\{1 + \frac{2}{v}H + \frac{H^2}{v^2}\right\}\,.
\end{aligned} \tag{67}$$

From (67) we see that the Higgs mass is given by

$$M_H = \sqrt{-2\mu^2} = \sqrt{2h}v\,. \tag{68}$$

And (67) also give us the couplings that can be seen in Fig. 6.

[9]The fields θ^i are the massless Goldstones.

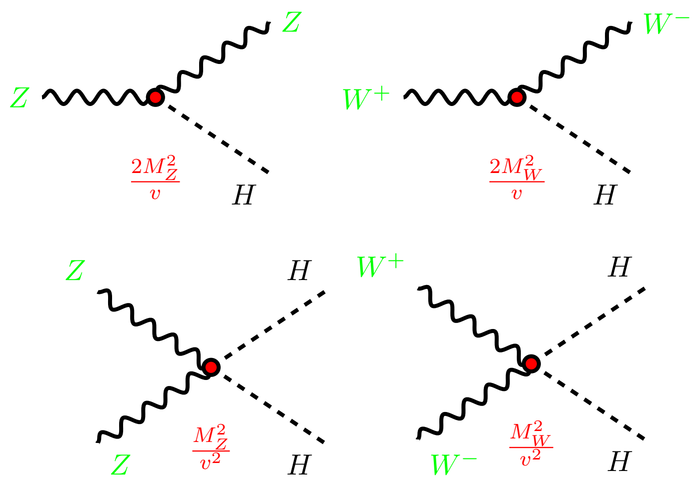

Figure 6: Higgs coupling to the gauge bosons.

3.3 Yukawa sector

Once we have introduced the Higgs doublet the right structures to give mass to the fermions can be formed. The forbidden structures by gauge invariance, that would give mass are of the form $\overline{\psi}\psi = \overline{\psi}_L\psi_R + \overline{\psi}_R\psi_L$, with the following quantum numbers: [10]

$$e_L \to (1,2,-\frac{1}{2}), \qquad \nu_{eL} \to (1,2,-\frac{1}{2}), \qquad u_L \to \left(3,2,\frac{1}{6}\right), \qquad d_L \to \left(3,2,\frac{1}{6}\right), \tag{69}$$
$$e_R \to (1,1,-1), \qquad \nu_{eR} \to (1,1,0), \qquad u_R \to \left(3,1,\frac{2}{3}\right), \qquad d_R \to \left(3,1,-\frac{1}{3}\right).$$

Note the left-handed fields form a doublet with the same quantum numbers, $L_L = \begin{bmatrix}\nu_{eL}\\ e_L\end{bmatrix}$ and $Q_L = \begin{bmatrix}u_L\\ d_L\end{bmatrix}$.

Since now we have a Higgs doublet with quantum numbers $\phi \to (1,2,\frac{1}{2})$ the following non-violating gauge symmetry structures can be formed:

$$\mathcal{L}_Y = -c_1[\bar{u},\bar{d}]_L \begin{bmatrix}\phi^{(+)}\\ \phi^{(0)}\end{bmatrix} d_R - c_2[\bar{u},\bar{d}]_L \begin{bmatrix}\phi^{(0)*}\\ -\phi^{(-)}\end{bmatrix} u_R - c_3[\bar{\nu}_e,\bar{e}]_L \begin{bmatrix}\phi^{(+)}\\ \phi^{(0)}\end{bmatrix} e_R + \text{h.c.}\,, \tag{70}$$

where the second term is the $\mathcal{C}$-conjugate scalar field, $\phi^c \equiv i\sigma_2\phi^*$, which in the unitary gauge we are working in has the form:

$$\phi^c = \frac{1}{\sqrt{2}}\begin{bmatrix}v+H(x)\\ 0\end{bmatrix}\,, \tag{71}$$

and the Lagrangian takes the form:

$$\mathcal{L}_Y = -\frac{1}{\sqrt{2}}(v+H)(c_1\bar{d}d + c_2\bar{u}u + c_3\bar{e}e)\,. \tag{72}$$

From where we can see that the mass of the fermions is a consequence of the vev of the Higgs doublet,

$$m_d = c_1\frac{v}{\sqrt{2}}\,, \qquad m_u = c_2\frac{v}{\sqrt{2}}\,, \qquad m_e = c_3\frac{v}{\sqrt{2}}\,. \tag{73}$$

The values of c_i are arbitrary, but the couplings of the fermions with the Higgs boson are fixed by the masses, as we can see in Fig. 7 and Eq. (74),

$$\mathcal{L}_Y = -\left(1+\frac{H}{v}\right)(m_d\bar{d}d + m_u\bar{u}u + m_e\bar{e}e)\,. \tag{74}$$

[10] The quantum numbers indicate C, L, Y = Q - T_3.

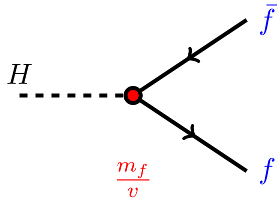

Figure 7: Higgs coupling to fermions.

3.4 Yukawa coupling for three generations

The existence of three generations of quarks and leptons is an experimental fact, as we have seen in Eq. (24). Since the particles of the second and third generation have the same quantum numbers and only differ in their masses, we can add more terms to the Lagrangian of Eq. (74)

$$\mathcal{L}_Y = -(\bar{\mathbf{Q}}'_L\mathbf{M}'_d\phi\mathbf{d}'_R + \bar{\mathbf{Q}}'_L\mathbf{M}'_u\phi^c\mathbf{u}'_R + \bar{\mathbf{L}}'_L\mathbf{M}'_l\phi\mathbf{l}'_R + \text{h.c})\,, \tag{75}$$

where $\mathbf{d}'_R$, $\mathbf{u}'_R$, $\mathbf{l}'_R$, $\bar{\mathbf{Q}}'_L$ and $\bar{\mathbf{L}}'_L$ are vectors in the 3-dimensional flavour space, and M'_d, M'_u and M'_l are the mass matrices. These non-diagonal mass matrices introduce a total of 54 parameters, [11] in addition of the non-conservation of lepton number. Since our Lagrangian is invariant under $[U(3)]^6$ we can perform transformations in the fermionic fields to reduce the number of parameters,

$$\begin{gathered}\mathbf{Q}'_L \to \mathbf{U}_Q\mathbf{Q}'_L \equiv \mathbf{Q}_L\,, \quad \mathbf{L}'_L \to \mathbf{U}_l\mathbf{L}'_L \equiv \mathbf{L}_L\,, \\ \mathbf{d}'_R \to \mathbf{U}_d\mathbf{d}'_R \equiv \mathbf{d}_R\,, \quad \mathbf{u}'_R \to \mathbf{U}_u\mathbf{u}'_R \equiv \mathbf{u}_R\,, \quad \mathbf{l}'_R \to \mathbf{U}_R\mathbf{l}'_R \equiv \mathbf{l}_R\,,\end{gathered} \tag{76}$$

which is equivalent to make a transformation in the mass matrices (for example for $\mathbf{M}'_d$):

$$\bar{\mathbf{d}}'_L\mathbf{M}'_d\mathbf{d}'_R \to \bar{\mathbf{d}}'_L\mathbf{U}_Q^\dagger\mathbf{M}'_d\mathbf{U}_d\mathbf{d}'_R = \bar{\mathbf{d}}_L\mathcal{M}_d\mathbf{d}_R\,. \tag{77}$$

Therefore it is as if the matrices $\mathbf{M}'_{a=d,u,l}$ were transformed as:

$$\begin{aligned}\mathbf{M}'_d &\to \mathbf{U}_Q^\dagger\mathbf{M}'_d\mathbf{U}_d\,, \\ \mathbf{M}'_u &\to \mathbf{U}_Q^\dagger\mathbf{M}'_u\mathbf{U}_u\,, \\ \mathbf{M}'_l &\to \mathbf{U}_L^\dagger\mathbf{M}'_l\mathbf{U}_R\,.\end{aligned} \tag{78}$$

It is convenient to choose a transformation such that the maximum number of parameters of the mass matrices is reduced, i.e, making them diagonal. But not all the matrices can be diagonalized simultaneously. As a result there will be two diagonal mass matrices and one hermitic mass matrix,

$$\begin{aligned}\frac{v}{\sqrt{2}}\mathbf{U}_Q^\dagger\mathbf{M}'_d\mathbf{U}_d &= \mathbf{M}_d\,, \\ \frac{v}{\sqrt{2}}\mathbf{U}_Q^\dagger\mathbf{M}'_u\mathbf{U}_d &= \mathcal{M}_u\,, \\ \frac{v}{\sqrt{2}}\mathbf{U}_L^\dagger\mathbf{M}'_l\mathbf{U}_R &= \mathcal{M}_l\,,\end{aligned} \tag{79}$$

where $\mathcal{M}_u$ and $\mathcal{M}_l$ are diagonal, positive defined matrices and $\mathbf{M}_d$ is an hermitian and positive defined matrix.

A non-diagonal mass matrix will imply a mixture between the up and down quarks. To diagonalize this matrix we can perform the transformation:

$$d_R \to Vd_R\,, \qquad d_L \to Vd_L. \tag{80}$$

[11] 3 rows x 3 columns x 2 (complex) x 3 matrices = 54 parameters.

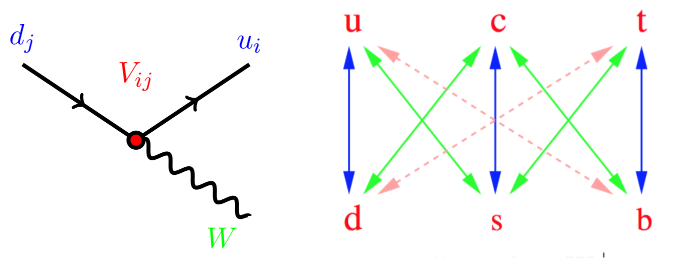

Figure 8: Flavour-changing interactions due to the CC part of the Lagrangian.

This $U(1)$ transformation is equivalent to diagonalize $M_d(M_d \to V^\dagger M_d V = \mathcal{M}_d)$. With that, the mass matrices of our Yukawa Lagrangian will be diagonal

$$\mathcal{L}_Y = -\left(1+\frac{H}{v}\right)\left(\mathbf{\overline{d}_L}\mathcal{M}_d\mathbf{d_R} + \mathbf{\overline{u}_L}\mathcal{M}_u\mathbf{u}_R + \mathbf{\overline{l}}_L\mathcal{M}_l\mathbf{l_R} + \text{h.c}\right). \tag{81}$$

The $\bar{u}u$ and $\bar{d}d$ pieces will remain invariant, while the $\bar{u}d$ and $\bar{d}u$ terms will be transformed according to Eq. (81):

$$\begin{aligned} &\bar{u}_L u_L \to \bar{u}_L u_L\,, && \bar{d}_L d_L \to \bar{d}_L V^\dagger V d_L = \bar{d}_L d_L\,, \\ &\bar{u}_L d_L \to \bar{u}_L V d_L\,, && \bar{d}_L u_L \to \bar{d}_L V^\dagger d_L\,. \end{aligned} \tag{82}$$

Having two terms (NC) that do not change flavour and two more (CC) that do change flavour (Fig. 8). In terms of the Lagrangians:

$$\mathcal{L}_{CC} = -\frac{2}{2\sqrt{2}}\left\{W_\mu^\dagger\left[\sum_{i,j}\bar{u}_i\gamma^\mu(1-\gamma_f)V_{ij}d_j + \sum_l \bar{\nu}_l\gamma^\mu(1-\gamma_5)l\right] + h.c.\right\}. \tag{83}$$

From where it can be seen that NC terms do not change flavour while CC terms do change flavour, via the so called Cabibbo-Kobayashi-Maskawa (CKM) matrix,

$$V = \begin{bmatrix} V_{ud} & V_{us} & V_{ub} \\ V_{cd} & V_{cs} & V_{cb} \\ V_{td} & V_{ts} & V_{tb} \end{bmatrix}. \tag{84}$$

3.5 Custodial Symmetry

The Custodial Symmetry, under the group $SU(2)_V = SU(2)_{L+R}$, is a global symmetry of the Higgs Lagrangian, $\mathcal{L}_S$ in the SM after the SSB and in the limit $g = g' \to 0$, that is, in the case in which gauge invariance is not imposed yet. Once gauge invariance is imposed, Custodial Symmetry becomes an approximate symmetry.

It is convenient to represent the Higgs doublet and its charge-conjugate into a 2×2 matrix [13, 14],

$$\Sigma \equiv \left[\tilde{\phi}, \phi\right] = \begin{bmatrix} \phi^{0*} & \phi^+ \\ -\phi^- & \phi^0 \end{bmatrix} = \frac{1}{\sqrt{2}}\Big(v + H(x)\Big)U(\vec{\varphi})\,, \tag{85}$$

being

$$U(\vec{\varphi}) = \exp\left(\frac{i}{v}\vec{\sigma}\vec{\varphi}(x)\right). \tag{86}$$

Introducing this notation, the Lagrangian of (55) can be written as:

$$\mathcal{L}_s = \frac{1}{2}\,\text{Tr}\left\{(D_\mu\Sigma)^\dagger D^\mu\Sigma\right\} - \frac{\lambda}{4}\left(\text{Tr}\left[\Sigma^\dagger\Sigma\right] - v^2\right) = \frac{v^2}{4}\,\text{Tr}\left\{(D_\mu U)^\dagger D^\mu U\right\} + \mathcal{O}(H/v)\,. \tag{87}$$

By writing $\mathcal{L}_s$ in this form, the existence of a global $SU(2)_L \times SU(2)_R$ symmetry is clear.

$$\Sigma \xrightarrow{SU(2)_L \times SU(2)_R} g_L \Sigma g_R^\dagger\,, \qquad g_X \in SU(2)_X\,, \tag{88}$$

but the ground state, $\langle 0|\,\Sigma\,|0\rangle = \frac{v}{\sqrt{2}} I_2$ is not invariant under this transformation unless the condition $g_L = g_R$ is imposed. Transformations which fulfill this conditions are said to belong to the custodial symmetry group $SU(2)_V$.

Thus the Lagrangian is characterized by the chiral symmetry breaking

$$SU(2)_L \otimes SU(2)_R \to SU(2)_V\,. \tag{89}$$

Being this the Custodial Symmetry. The $SU(2)_L$ group is a local gauge symmetry, while only the $U(1)_Y$ subgroup of $SU(2)_R$ is gauged. The $SU(2)_R$ symmetry is broken at $\mathcal{O}(g')$.

The three broken generators after the chiral symmetry breaking give rise to the three massless Goldstone bosons, which can be eliminated from $\mathcal{L}$. Going to the unitary gauge, it can be seen that the masses of the three gauge bosons, $W^\pm, Z$ are generated through the covariant derivatives.

This symmetry gives the relation between the masses of the W and Z bosons that we have previously seen in Section 3.2

$$\rho = \frac{M_W^2}{M_Z^2 \cos^2\theta_\mathrm{w}} = \frac{v^2[T(T+1) - Y^2]}{2v^2Y^2} = 1\,, \tag{90}$$

where we have written the masses in terms of the eigenvalues of the operators of the involved groups ($T = \frac{1}{2} = Y$).

To finish this section, recall that, in addition to the symmetry breaking due to the covariant derivative there are also breaking terms due to radiative corrections of massive fermions, being specially important the top-bottom quark doublet.

4 Higgs singlet extension

4.1 The model

In this section we will describe the most simple extension of the scalar sector of the SM, in which a real bosonic singlet, neutral under all quantum numbers of the SM gauge group, is added to the SM Higgs doublet [14, 15].

We have the freedom of adding a real singlet, φ, to the Lagrangian of (55) that we have used in our discussion about the Higgs boson. The addition of such singlet (in fact we could add as many sclar singlets as we desire) is motivated from the relation between the $W^\pm$ and Z masses of Eq. (90), or which is the same, the SM prediction $M_W = M_Z \cos\theta_\mathrm{w}$. In general, extending the scalar sector with different fields, ϕ_i belonging to different represenations (T_i, Y_i) will yield into a different form of ρ at tree level [14],

$$\rho = \frac{\sum_i v_i^2[T_i(T_i+1) - Y_i^2]}{2\sum_i v_i^2 Y_i^2}\,. \tag{91}$$

Remember from Section 3.5 $\rho = 1$ for the SM. By adding an arbitrary number of singlet fields ($Y_i = T_i = 0$) this result won't change, and the SM's relation between the boson masses will also hold.

This extension with one extra singlet will be described, studying the constraints of the parameters and comparing with the current LHC data by performing a χ^2 test. We will study the possibilities or *scenarios* depending on the mass of the discovered Higgs (of 125 GeV).

The Lagrangian of a model with an extra singlet is:

$$\mathcal{L} = (D^\mu\phi)^\dagger(D_\mu\phi) + \frac{1}{2}\partial_\mu\varphi\partial^\mu\varphi - V(\phi,\varphi)\,. \tag{92}$$

With the potential taking the most general renormalizable form (dimension ≤ 4):

$$V(\phi,\varphi) = \mu'^2(\phi^\dagger\phi) + h'(\phi^\dagger\phi)^2 + (a'\varphi + b'\varphi^2 + c'\varphi^3 + d'\varphi^4) + (\phi^\dagger\phi)(A'\varphi + B'\varphi^2)\,. \tag{93}$$

Since the fields are not physical themselves, and to partially recover the results of the SM we can make a redefinition of the fields, $\varphi \to \varphi + \langle\varphi\rangle$, such that φ doesn't get a vev, $\langle 0|\,\varphi\,|0\rangle = 0$. Performing this transformation the potential takes the form:

$$
\begin{aligned}
V(\phi,\varphi) = &\Big(\mu'^2 + A'\langle\varphi\rangle + B'\langle\varphi\rangle^2\Big)(\phi^\dagger\phi) + h'(\phi^\dagger\phi)^2 + \Big(a' + 2b'\langle\varphi\rangle + 3c'\langle\varphi\rangle^2 + 4d'\langle\varphi\rangle^3\Big)\varphi \\
&+ \Big(b' + 3c'\langle\varphi\rangle + 6d'\langle\varphi\rangle^2\Big)\varphi^2 + \Big(c' + 4d'\langle\varphi\rangle\Big)\varphi^3 + d'\varphi^4 \\
&+ (\phi^\dagger\phi)\Big((A' + 2B'\langle\varphi\rangle)\varphi + B'\varphi^2\Big) + \Big(a'\langle\varphi\rangle + b'\langle\varphi\rangle^2 + c'\langle\varphi\rangle^3 + d'\langle\varphi\rangle^4\Big) \\
&= \mu^2(\phi^\dagger\phi) + h(\phi^\dagger\phi)^2 + (a\varphi + b\varphi^2 + c\varphi^3 + d\varphi^4) + (\phi^\dagger\phi)(A\varphi + B\varphi^2) + V_0'\,.
\end{aligned} \tag{94}
$$

with $V_0' = a'\langle\varphi\rangle + b'\langle\varphi\rangle^2 + c'\langle\varphi\rangle^3 + d'\langle\varphi\rangle^4$.

As we did in the previous section, for the potential to behave correctly it has to be:

- increasing: $h > 0$, $d > 0$ and $B > 0$.
- bounded (to have minima): $\det H > 0$, where H is the Hessian matrix.

To find the minima of the potential

$$
\begin{aligned}
\frac{\partial V}{\partial|\phi|} &= 0 \to 2\mu^2|\phi| + 4h|\phi|^3 + 2|\phi|(A\varphi + B\varphi^2)\,, \\
\frac{\partial V}{\partial\varphi} &= 0 \to a + 2b\varphi + 3c\varphi^2 + 4d\varphi^3 + |\phi|^2(A + 2B\varphi) = 0\,.
\end{aligned} \tag{95}
$$

Doing that, the minima of (95) can take two different forms:

1. $|\phi| = 0$, $a = 0$,
2. $4h|\phi|^2 = -2\mu^2 \to |\phi| = \sqrt{-\frac{\mu^2}{2h}} \equiv \frac{v}{\sqrt{2}}$, $a = \frac{\mu^2}{2h}A = -\frac{v^2}{2}A$.

If we study the critical points, we have for **1**:

$$
|H| = \begin{bmatrix} 2\mu^2 & 0 \\ 0 & 2b \end{bmatrix} = 4b\mu^2 < 0 \to \text{maximum} \tag{96}
$$

And for **2**:

$$
|H| = \begin{bmatrix} -4\mu^2 & 2A\sqrt{\frac{-\mu^2}{2h}} \\ 2A\sqrt{\frac{-\mu^2}{2h}} & 2b - \frac{B\mu^2}{h} \end{bmatrix} = 4\mu^2\Big(-2b + \frac{B\mu^2}{h} + \frac{A^2}{2h}\Big) > 0 \to \text{minimum} \tag{97}
$$

where, as in the SM $\mu^2 < 0$, and in (97) we have imposed the condition $|H| > 0$ for the potential to have minima. Now we are in a situation similar than the one in Section 3 and we would have:

$$
\langle 0|\,\phi\,|0\rangle = \begin{bmatrix} 0 \\ \frac{v}{\sqrt{2}} \end{bmatrix}\,, \qquad \langle 0|\,\varphi\,|0\rangle = 0\,. \tag{98}
$$

As before, considering excitations over the ground state and in the unitary gauge, we can parametrize the fields as:

$$
\begin{aligned}
\phi(x) = e^{i\frac{\sigma_i}{2}\theta^i(x)}\frac{1}{\sqrt{2}}\begin{bmatrix} 0 \\ v + H(x) \end{bmatrix} &\xrightarrow{\text{unitary gauge}} \frac{1}{\sqrt{2}}\begin{bmatrix} 0 \\ v + H(x) \end{bmatrix}\,, \\
\varphi(x) &\xrightarrow{\text{unitary gauge}} \varphi(x)\,.
\end{aligned} \tag{99}
$$

Once this parametrization is done, we can look at the kinetic terms of the Lagrangian,

$$(D^\mu\phi^\dagger)(D_\mu\phi) + (\partial^\mu\varphi)(\partial_\mu\varphi) = \frac{1}{2}\partial_\mu H\partial^\mu H + (v+H)^2\left(\frac{g^2}{4}W_\mu^\dagger W_\mu + \frac{g^2}{8\cos^2\theta_{\rm w}}Z^\mu Z_\mu\right) + (\partial^\mu\varphi)(\partial_\mu\varphi)\,. \tag{100}$$

And for the potential term:

$$\begin{aligned} V =& \underbrace{-\frac{1}{4}hv^4 + V_0'}_{V_0} + \underbrace{(hvH^3 + \frac{h}{4}H^4)}_{\text{Higgs self-interactions}} + \underbrace{(c\varphi^3 + d\varphi^4)}_{\varphi\text{ self interactions}} \\ &+ \underbrace{\frac{1}{2}M_H^2H^2 + \frac{1}{2}M_\varphi^2\varphi^2 + Av\varphi H}_{\text{Mass terms}} + \underbrace{Bv\varphi^2H + \frac{1}{2}AH^2\varphi + \frac{1}{2}BH^2\varphi^2}_{\text{H-}\varphi\text{ interaction}}\,, \end{aligned} \tag{101}$$

with $M_H^2 = -2\mu^2$ and $M_\varphi^2 = 2b + Bv^2$.

From the form of the potential we can see that there will be new interactions between the SM Higgs boson and the new scalar, and self-interactions between the bosons. In addition, we can note that we have a mixture between the quadratic terms of H and φ. This means the mass eigenstates of the fields are not H and φ, but a mixture of them. Such mixture can be parametrized by a rotation,

$$\begin{bmatrix} h_1 \\ h_2 \end{bmatrix} = \begin{bmatrix} \cos\theta & \sin\theta \\ -\sin\theta & \cos\theta \end{bmatrix} \begin{bmatrix} H \\ \varphi \end{bmatrix}\,, \tag{102}$$

with mixing angle $\theta = [0,\pi]$,

$$\tan 2\theta = \frac{2Av}{M_H^2 - M_\varphi^2}\,, \tag{103}$$

and

$$m_{h_{1,2}}^2 = \frac{M_H^2 + M_\varphi^2}{2} \pm \frac{|M_H^2 - M_\varphi^2|}{2}\sqrt{1+\tan^2 2\theta}\,. \tag{104}$$

Now $h_{1,2}$ are the scalar fields with masses m_{h_1} and m_{h_2}, and being h_1 the heavy Higgs, $m_{h_1}^2 > m_{h_2}^2$.

In terms of the fields $h_{1,2}$ the interaction potential takes the form:

$$\begin{aligned} V_{\rm int} =& h_1^3\Big(hv\cos^3\theta + c\sin^3\theta + Bv\sin^2\theta\cos\theta + \frac{A}{2}\sin\theta\cos^2\theta\Big) \\ &+ h_1^4\Big(\frac{h}{4}\cos^4\theta + d\sin^4\theta + \frac{B}{2}\sin^2\theta\cos^2\theta\Big) \\ &+ h_2^3\Big(-hv\sin^3\theta + c\cos^3\theta - Bv\sin\theta\cos^2\theta + \frac{A}{2}\sin^2\theta\cos\theta\Big) \\ &+ h_2^4\Big(\frac{h}{4}\sin^4\theta + d\cos^4\theta + \frac{B}{2}\sin^2\theta\cos^2\theta\Big) \\ &+ h_1^2h_2\Big(-3hv\sin\theta\cos^2\theta + 3c\sin^2\theta\cos\theta + Bv\sin\theta(2-3\sin^2\theta) + \frac{A}{2}\cos\theta(1-3\sin^2\theta)\Big) \\ &+ h_1h_2^2\Big(3hv\sin^2\theta\cos\theta + 3c\sin\theta\cos^2\theta + Bv\cos\theta(1-3\sin^2\theta) + \frac{A}{2}\sin\theta(3\sin^2\theta-2)\Big) \\ &+ h_1^3h_2\Big(-h\sin\theta\cos^3\theta + 4d\sin^3\theta\cos\theta + \frac{B}{4}\sin 4\theta\Big) \\ &+ h_1h_2^3\Big(-h\sin^3\theta\cos\theta + 4d\sin\theta\cos^3\theta - \frac{B}{4}\sin 4\theta\Big) \\ &+ h_1^2h_2^2\Big(\sin^2\theta\cos^2\theta\Big(\frac{3}{2}h + 6d - 3B\Big) + \frac{B}{2}\Big)\,. \end{aligned} \tag{105}$$

From where it can be seen there are self-interactions of the bosons and interaction between h_1 and h_2, as we can see in Fig. 9.

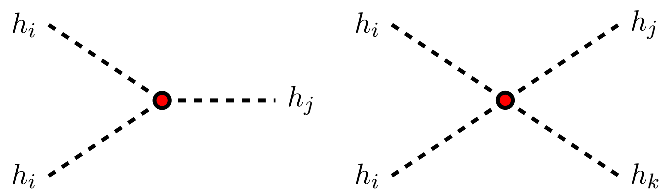

Figure 9: Self interactions of $h_{1,2}$ (with $i = j = k$) and different interactions between the two Higgs-like particle of the model (with $i = k \neq j$ and $j = k \neq i$).

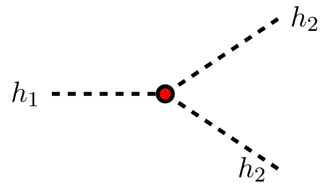

Figure 10: Decay of the heavy Higgs-like particle, h_1, into two light Higgs-like particles, h_2h_2.

4.2 Phenomenology and global fits

Since the field φ is a singlet under $SU(2)_L \otimes U(1)_Y$ transformations, it does not couple to fermions and gauge bosons and the coupling of the scalars $h_{1,2}$ to those particles will only be through their doublet component, H [14].

But there is a new ingredient within this model. Since we have made the diagonalization of the mass matrix the Yukawa Lagrangian is slightly different,

$$\mathcal{L}_{\rm Y} = -\frac{1}{\sqrt{2}}\Big(1 + \frac{h_1\cos\theta - h_2\sin\theta}{v}\Big)\Big(c_2\bar{d}d + c_2\bar{u}u + c_3\bar{e}e\Big)\,. \tag{106}$$

And, even though the masses won't change, the interaction vertices will do, having the couplings $\frac{m_f\cos\theta}{v}$ and $\frac{m_f\sin\theta}{v}$.

Depending on the parameters of the potential we will have a "suppressed" Higgs and another "allowed". At first sight, and taking into account that our observations seem to be compatible with the existence of just one Higgs boson, the suppression must be important.

As a consequence, there will be a universal reduction of the couplings with respect to the SM.

$$\begin{aligned} \kappa_V^{h_1} &\equiv g_{h_1VV}/g_{HVV}^{SM} = \cos\theta\,, \qquad & \kappa_f^{h_1} &\equiv y_{h_1ff}/y_{Hff}^{SM} = \cos\theta\,, \\ \kappa_V^{h_2} &\equiv g_{h_2VV}/g_{HVV}^{SM} = -\sin\theta\,, \qquad & \kappa_f^{h_2} &\equiv y_{h_2ff}/y_{Hff}^{SM} = -\sin\theta\,. \end{aligned} \tag{107}$$

The branching ratios and strengths of the two Higgs-like particles will be different. The lighter scalar will have the same decay branching ratios as the SM Higgs boson, $\text{BR}(h_2 \to X) = \text{BR}\ (H \to X)_{SM}$ and $\Gamma_{h_2}/\Gamma_H^{SM} = \sin^2\theta$, while the heaviest scalar boson can also have the contribution of $h_1 \to h_2h_2$ (Fig. 10) if allowed, i.e. if $m_{h_1} > 2m_{h_2}$.

Such process will have a decay width of:

$$\Gamma_{h_1\to h_2h_2} = \frac{|\widetilde{\mu}|^2}{8\pi m_{h_1}}\sqrt{1 - \frac{4m_{h_2}^2}{m_{h_1}^2}}\,, \tag{108}$$

with

$$\widetilde{\mu} = (3hv\sin^2\theta\cos\theta + 3c\sin\theta\cos^2\theta + Bv\cos\theta(1 - 3\sin^2\theta) + \frac{A}{2}\sin\theta(3\sin^2\theta - 2)\,. \tag{109}$$

And we have,

$$\Gamma_{h_1} = \Gamma_{SM}\cos^2\theta + \underbrace{\Gamma_{h_1\to h_2h_2}}_{\text{if allowed}}\,, \tag{110}$$
$$\Gamma_{h_2} = \Gamma_{SM}\sin^2\theta\,.$$

Depending on the mass of these bosons, there will be three different possibilities or *scenarios*. First of all, the most simple possibility is that the 125 GeV Higgs that we have found is the light Higgs (*heavy scenario*). This possibility is pretty simple since all the strengths will be the same as in the SM but reduced by a factor of $\sin\theta$ and there will not be any new process contributing such as the decay of Fig. 10. The possibility of the found Higgs being the heavy boson, is slightly more complicated because, in addition of the suppressing factor $\cos\theta$ the new decay of $h_1 \to h_2h_2$ may be present.

To analyze these possibilities, we will consider the Higgs signal strengths and will perform a phenomenological analysis based on the minimization of the χ^2 function. Details on the statistical treatment on the data, as well as the experimental data used can be found in Appendix A.

4.2.1 Heavy scenario

It is easy to see that, for the heavy scenario the ratio of the cross sections for all the channels is

$$\frac{\sigma(pp\to h_2Y)}{\sigma(pp\to HY)_{SM}} = \sin^2\theta\,. \tag{111}$$

And for the branching ratios

$$\frac{\mathrm{BR}(h_2\to X)}{\mathrm{BR}(H\to X)_{SM}} = \frac{\Gamma(h_2\to X)}{\Gamma_{h_2}}\frac{\Gamma_{H,SM}}{\Gamma(H\to X)_{SM}} = \frac{\sin^2\theta}{1}\frac{1}{\sin^2\theta} = 1\,. \tag{112}$$

So all the Higgs signal strengths, defined as $\mu = \frac{\sigma(pp\to h_2Y)}{\sigma(pp\to HY)_{SM}}\frac{\mathrm{BR}(h_2\to X)}{\mathrm{BR}(H\to X)_{SM}}$ are the same, $\mu = \sin^2\theta$.

Now, we can perform the minimization of the χ^2 function, defined as the difference between the strengths of our model and the experimental ones over the experimental uncertainty, as described in the Appendix A, getting a best-fit value for the $\sin\theta$ with a 1σ uncertainty of:

$$\sin\theta = 0.99 \pm 0.01\,, \tag{113}$$

obtaining a value of the $\chi^2/$ d.o.f. of 0.62.

As it can be seen in the left panel of Fig. 11, using this result we can compare the allowed ranges at 1σ and 2σ with the experimental values, obtaining a good agreement at this level of significance. Due to the value of $\sin\theta$, very close to 1, the strengths obtained are almost the ones predicted by the SM.

4.2.2 Light scenario

This case is very similar to the heavy scenario, with the difference that now an additional decay, as described in (108) and in Fig. 10 can be present. Now, for the branching ratios:

$$\frac{\mathrm{BR}(h_1\to X)}{\mathrm{BR}(H\to X)_{SM}} = \frac{\Gamma_{h_1\to X}}{\Gamma_{h_1}}\frac{\Gamma_{H,SM}}{\Gamma_{H\to X,SM}} = \frac{\cos^2\theta\Gamma_{H,SM}}{\cos^2\theta\Gamma_{H,SM}+\Gamma_{h_1\to h_2h_2}} = \frac{1}{1+\frac{\Gamma_{h_1\to h_2h_2}}{\cos^2\theta\Gamma_{H,SM}}}\,. \tag{114}$$

And all the cross section ratios involving the Higgs scalars are identical, $\frac{\sigma}{\sigma_{SM}} = \cos^2\theta$, yielding into identical strengths,

$$\mu = \cos^2\theta \times \frac{1}{1+\frac{\Gamma_{h_1\to h_2h_2}}{\cos^2\theta\Gamma_{H,SM}}} = \frac{\cos^4\theta}{\cos^2\theta+\frac{\Gamma_{h_1\to h_2h_2}}{\Gamma_{H,SM}}}\,. \tag{115}$$

As before, we can perform a χ^2 minimization in order to get the best fit values of the parameters we have (in this case, $\cos\theta$ and $\Gamma_{h_1\to h_2h_2}$). The best-fit parameters are obtained for the case in which

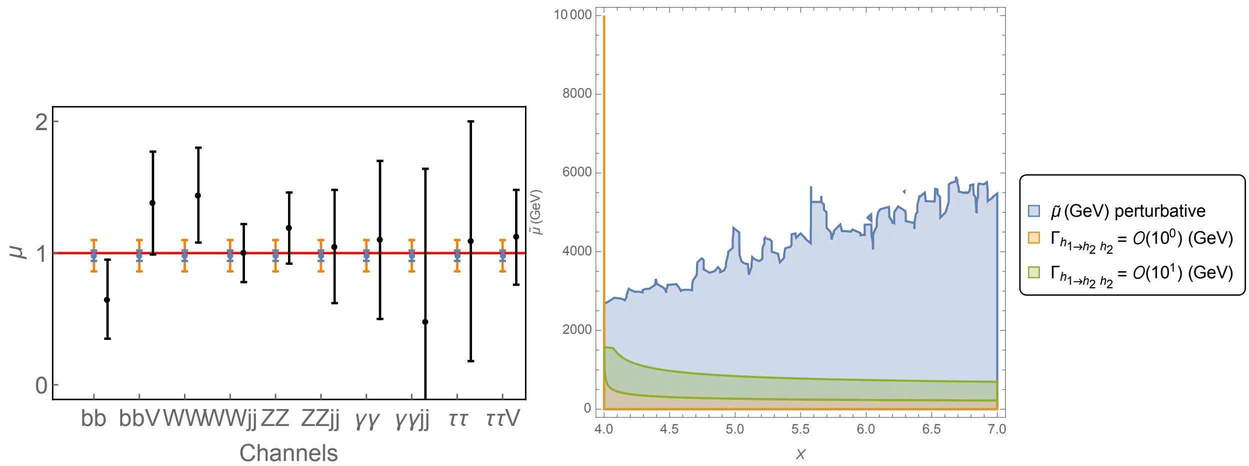

Figure 11: **Left:** Allowed ranges for the Higgs signal strengths obtained for the fit (113) at 1σ (blue) and 2σ (orange), together with the experimental data of ATLAS and CMS with 1σ errors (black) for the heavy scenario. **Right:** Value of the coupling constant $\widetilde{\mu}$ and X ($X = \frac{m_{h_2}^2}{m_{h_1}^2}$) for which the process is perturbative (blue) and for which the decay width is of the order of magnitude $\mathcal{O}(10^0)$ GeV (orange) and $\mathcal{O}(10^1)$ GeV (green).

the decay width of h_1 into h_2h_2 is very suppressed (and considered to be zero). In this case, we reproduce the results of the previous section (now $\cos\theta = 0.99 \pm 0.01$), with a redefinition of the angle, $\theta \to \theta + \frac{\pi}{2}$. If we require a contribution to the decay width of $\Gamma_{h_1 \to h_2 h_2}$ to be considerable, the value of the parameter quantizing our fit, $\chi^2/\text{d.o.f.}$, increases as $\Gamma_{h_1 \to h_2 h_2}$ while the value of $\cos\theta$ that best fits does not change.

Currently, there is no experimental evidence of a light scalar with the characteristics of h_2, which would indicate $\Gamma_{h_1 \to h_2 h_2} \approx 0$, ruling out this scenario, as the best fit values of our minimization seem to indicate. If evidence of a particle with the features of the light boson described in this section was found, the function χ^2 would have to be modified in order to include these experimental results, having as a consequence the modification of our fit.

Assuming the decay $h_1 \to h_2 h_2$ exists and is of significance, the parameters of the decay width would need to meet perturbative constraints. In the right panel of Fig. 11 it can be seen the region where the coupling constant, $\widetilde{\mu}$, is perturbative and for which range of mass, given as the square fraction between the Higgs masses, $X = \frac{m_{h_2}^2}{m_{h_1}^2}$. [12] The perturbative region is obtained comparing the tree level vertex with the one loop correction, as explained in Appendix C. Other constraints, which can be more restrictive, may be obtained from other methods. In this figure it also can be seen the values of $\widetilde{\mu}$ and X that will give an hypothetical decay width of order of magnitude $\mathcal{O}(10^0)$ GeV (orange) and $\mathcal{O}(10^1)$ GeV (green).

5 The two-Higgs doublet model

The existence of a Higgs-like boson with mass around 125 GeV is a fact supported by the last LHC data. The SM is the most simple model that explains the existence of this particle, but nothing forbids us from building a more complicated model, such as the one studied in this section, the two-Higgs double model (2HDM), which will both include all the features of the SM as well as some new ingredients of new physics, like new sources of CP violation or dark matter candidates.

In this section we will describe the basic ingredients of the model, i.e. the scalar potential and the process of SSB, identifying the two CP-even Higgs-like particles of the model and the CP-odd particle in the CP conserving limit. Later, we will see how the alignment in flavour space is required in order to avoid FCNCs and the consequences of the alignment. In Section 5.5 the available LHC data will be analyzed in the context of the model.

[12]Note the mass of the lightest Higgs is constrained to be $m_{h_1} \geq 2m_{h_2}$.

5.1 The model. Scalar potential and symmetry breaking

In this model, in addtition to the usual ingredients of the SM, a new doublet with the same quantum numbers as the SM Higgs is added [16, 17],

$$\phi_1 = \begin{bmatrix} \phi_1^{(+)} \\ \phi_1^{(0)} \end{bmatrix}, \qquad \phi_2 = \begin{bmatrix} \phi_2^{(+)} \\ \phi_2^{(0)} \end{bmatrix}. \tag{116}$$

First of all, let's look at the ρ parameter defined in Eq. (90),

$$\rho = \frac{\frac{1}{2}v_1^2 + \frac{1}{2}v_2^2}{2(\frac{1}{4}v_1^2 + \frac{1}{4}v_2^2)} = 1\,. \tag{117}$$

Again, we still have the same prediction relating the mass of the W and the Z bosons of the SM. [13]

The procedure to follow is the usual. We will build the most general renormalizable potential that respect the symmetries. The minimization of this potential will give us a value for the vev of the doublets, and considering excitations over the vacuum in a convenient gauge the phenomenology and the interesting ingredients of the model will be studied.

Before minimizing the potential, we should take into account the general form of the vev of the doublets:

$$\langle 0|\,\phi_1\,|0\rangle = \frac{1}{\sqrt{2}}\begin{bmatrix} 0 \\ v_1 e^{i\theta_1} \end{bmatrix}, \qquad \langle 0|\,\phi_2\,|0\rangle = \frac{1}{\sqrt{2}}\begin{bmatrix} 0 \\ v_2 e^{i\theta_2} \end{bmatrix}. \tag{118}$$

Since we are allowed to make an arbitrary $U(1)$ transformation, $\phi_i \to \phi_i' = \phi_i e^{-i\theta_1}$, one of the phases can be eliminated,

$$\langle 0|\,\phi_1\,|0\rangle = \frac{1}{\sqrt{2}}\begin{bmatrix} 0 \\ v_1 \end{bmatrix}, \qquad \langle 0|\,\phi_2\,|0\rangle = \frac{1}{\sqrt{2}}\begin{bmatrix} 0 \\ v_2 e^{i\theta_2-\theta_1} \end{bmatrix} = \frac{1}{\sqrt{2}}\begin{bmatrix} 0 \\ v_2 e^{i\varepsilon} \end{bmatrix}. \tag{119}$$

Furthermore, it is convenient to perform a $SU(2)$ transformation in the scalar space (ϕ_1, ϕ_2), and work in the so called Higgs basis (Φ_1, Φ_2), in which only one of the doublets acquire a vev,

$$\begin{bmatrix} \Phi_1 \\ -\Phi_2 \end{bmatrix} = \frac{1}{v}\begin{bmatrix} v_1 & v_2 \\ v_2 & -v_1 \end{bmatrix}\begin{bmatrix} \phi_1 \\ e^{-i\varepsilon}\phi_2 \end{bmatrix} = \frac{1}{v}\begin{bmatrix} v_1\phi_1 + e^{-i\varepsilon}v_2\phi_2 \\ v_2\phi_1 - e^{-i\varepsilon}v_1\phi_2 \end{bmatrix}, \tag{120}$$

with $v^2 = v_1^2 + v_2^2$

In this basis, the vev of the doublets, are:

$$\langle 0|\,\Phi_1\,|0\rangle = \frac{1}{\sqrt{2}}\begin{bmatrix} 0 \\ v \end{bmatrix}, \qquad \langle 0|\,\Phi_2\,|0\rangle = \begin{bmatrix} 0 \\ 0 \end{bmatrix}. \tag{121}$$

Just one of the doublets would acquire the same vev as in the SM (Section 3), while the vev of the second one would be zero. Following the procedure of Sections 3 and 4, we consider excitations over the vacuum,

$$\Phi_1 = \begin{bmatrix} G^+ \\ \frac{1}{\sqrt{2}}(v + S_1 + iG^0) \end{bmatrix}, \qquad \Phi_2 = \begin{bmatrix} H^+ \\ \frac{1}{\sqrt{2}}(S_2 + iS_3) \end{bmatrix}. \tag{122}$$

The first doublet, Φ_1 looks similar to the SM-Higgs doublet and the second one is just a copy of Φ_1 with 0 vev. We can see that, in addition to the three Goldstone fields, $G^\pm$ and G^0, there are five physical degrees of freedom in the scalar sector: two charged fields, $H^\pm$, two CP-even neutral $\{S_i\}_{i=1,2}$ and one CP-odd neutral, S_3.

In the Higgs basis the potential takes the form [14],

[13] This relation will also hold in a generalized model in which an arbitrary number of doublets is added.

$$\begin{aligned} V = & \mu_1^2(\Phi_1^\dagger\Phi_1) + \mu_2^2(\Phi_2^\dagger\Phi_2) + [\mu_3\Phi_1^\dagger\Phi_2 + \mu_3^*\Phi_2^\dagger\Phi_1] \\ & +\lambda_1(\Phi_1^\dagger\Phi_1)^2 + \lambda_2(\Phi_2^\dagger\Phi_2)^2 + \lambda_3(\Phi_1^\dagger\Phi_1)(\Phi_2^\dagger\Phi_2) + \lambda_4(\Phi_1^\dagger\Phi_2)(\Phi_2^\dagger\Phi_1) \\ & +\Big[(\lambda_5\Phi_1^\dagger\Phi_2 + \lambda_6\Phi_1^\dagger\Phi_1 + \lambda_7\Phi_2^\dagger\Phi_2)(\Phi_1^\dagger\Phi_2) + \text{h.c.}\Big]\,. \end{aligned} \tag{123}$$

Due to the hermiticy of the potential, the parameters μ_1, μ_2, λ_1, λ_2, λ_3 and λ_4 are real, so there are a total of 14 real independent parameters. Proceeding with the minimization of the potential of Eq. (123) with the form of the vevs of Eq. (122) we find:

$$\left.\begin{aligned} \frac{\partial V}{\partial \Phi_1} = 0 \\ \frac{\partial V}{\partial \Phi_2} = 0 \end{aligned}\right\} \to \mu_1^2 = -\lambda_1 v^2\,, \quad \mu_3 = -\frac{\lambda_6 v^2}{2}\,. \tag{124}$$

And the potential, decomposed into mass, cubic and quadratic term takes the form,

$$V = -\frac{1}{4}\lambda_1 v^4 + V_2 + V_3 + V_4\,, \tag{125}$$

with

$$V_2 = M_{H^\pm}^2 H^+H^- + \frac{1}{2}\begin{bmatrix} S_1, & S_2, & S_3 \end{bmatrix} \mathcal{M} \begin{bmatrix} S_1 \\ S_2 \\ S_3 \end{bmatrix}\,, \tag{126}$$

being $M_{H^\pm}^2$ function of the parameters of the potential and the mass matrix of S_i non-diagonal,

$$M_{H^\pm}^2 = \mu_2^2 + \frac{1}{2}\lambda_3 v^2\,, \tag{127}$$

$$\mathcal{M} = \begin{bmatrix} 2\lambda_1 v^2 & v^2\lambda_6^R & -v^2\lambda_6^I \\ v^2\lambda_6^R & M_{H^\pm}^2 + v^2(\frac{\lambda_4}{2} + \lambda_5^R & -v^2\lambda_5^I \\ -v^2\lambda_6^I & -v^2\lambda_5^I & M_{H^\pm}^2 + v^2\left(\frac{\lambda_4}{2} - \lambda_5^R\right) \end{bmatrix}. \tag{128}$$

with $\lambda_i^R = \mathrm{Re}(\lambda_i)$ and $\lambda_i^I = \mathrm{Im}(\lambda_i)$.

This indicates us that the Goldstone bosons, $G^\pm$ and G^0 are massless fields, while from the matrix of Eq. (128) we can see that the neutral fields do have mass. It can also be seen that their mass eigenstates are not S_i but a mixture of them. Since the matrix $\mathcal{M}$ contains imaginary terms, the resulting mass eigenstates will not have a definite CP parity.

The matrix $\mathcal{M}$ is diagonalized by an orthogonal rotation, $\mathcal{R}$ that relates the fields $\{S_i\}_{i=1,2,3}$ with the mass eigenstates $\varphi_i^0 = \{h(x), H(x), A(x)\}$:

$$\mathcal{M} = \mathcal{R}^T \begin{bmatrix} M_h^2 & 0 & 0 \\ 0 & M_H^2 & 0 \\ 0 & 0 & M_A^2 \end{bmatrix} \mathcal{R}\,, \qquad \begin{bmatrix} h \\ H \\ A \end{bmatrix} = \mathcal{R} \begin{bmatrix} S_1 \\ S_2 \\ S_3 \end{bmatrix}. \tag{129}$$

Matching the traces of (128) and (129) it can be seen:

$$M_h^2 + M_H^2 + M_A^2 = 2M_{H^\pm}^2 + v^2(2\lambda_1 + \lambda_4)\,. \tag{130}$$

Before continuing let's count the degrees of freedom of our potential. The minimization of the potential in Eq. (124) allows us to express μ_1, μ_3 in terms of v, λ_6. Furthermore, since we have freedom to rephase Φ_2, only the relative phases among λ_5, λ_6 and λ_7 are relevant, being just two of them independent. Therefore, we can parametrize the potential with 11 parameters (v, μ_2, $|\lambda_{1\ldots7}|$, $\arg(\lambda_5\lambda_6^*)$ and $\arg(\lambda_5\lambda_7^*)$.

In the CP conserving limit ($\lambda_5^I = \lambda_6^I = \lambda_7^I = 0$), the CP admixture disappears and S_3 does not mix with other neutral fields. The scalar spectrum contains a CP-odd field, $A = S_3$, and two CP-even fields, h and H, which are a mixture of S_1 and S_2,

$$\begin{bmatrix} h \\ H \end{bmatrix} = \begin{bmatrix} \cos\tilde{\alpha} & \sin\tilde{\alpha} \\ -\sin\tilde{\alpha} & \cos\tilde{\alpha} \end{bmatrix} \begin{bmatrix} S_1 \\ S_2 \end{bmatrix}. \tag{131}$$

We choose the convention $M_h \leq M_H$ and $0 \leq \tilde{\alpha} \leq \pi$, so that $\sin\tilde{\alpha}$ is positive.

In this case, the masses of the scalar fields are:

$$M_h^2 = \frac{1}{2}(\Sigma - \Delta)\,, \quad M_H^2 = \frac{1}{2}(\Sigma + \Delta)\,, \quad M_A^2 = M_{H^\pm}^2 + v^2\Big(\frac{\lambda_4}{2} - \lambda_5^R\Big)\,, \tag{132}$$

with

$$\begin{aligned} \Sigma &= M_{H^\pm}^2 + v^2\left(2\lambda_1 + \frac{\lambda_4}{2} + \lambda_5^R\right)\,, \\ \Delta &= \sqrt{\left[M_{H^\pm}^2 + v^2(-2\lambda_1 + \frac{\lambda_4}{2} + \lambda_5^R)\right]^2 + 4v^2(\lambda_6^R)^2}\,, \\ \tan\tilde{\alpha} &= \frac{M_h^2 - 2\lambda_1 v^2}{\lambda_6^R v^2}\,. \end{aligned} \tag{133}$$

Finally and for completeness, let's consider the cubic and quartic terms of the potential of Eq. (125) in the most general case in which CP is not conserved.

$$\begin{aligned} V_3 = {} & vH^+H^-(\lambda_3 S_1 + \lambda_7^R S_2 - \lambda_7^I S_3) - \frac{1}{2}v\lambda_7^I S_3^3 - \frac{1}{2}v\lambda_7^I S_2^2 S_3 - \frac{3}{2}v\lambda_6^I S_1^2 S_3 \\ & + \lambda_1 v S_1^3 + \frac{1}{2}v\lambda_7^R S_2^3 + \frac{3}{2}v\lambda_6^R S_1^2 S_2 + \frac{1}{2}v\Big(2\lambda_5^R + \lambda_3 + \lambda_4\Big)S_1 S_2^2 \\ & - \frac{1}{2}v\Big(2\lambda_5^R - \lambda_3 - \lambda_4\Big)S_1 S_3^2 + \frac{1}{2}v\lambda_7^R S_2 S_3^2 - 2v\lambda_5^I S_1 S_2 S_3\,, \end{aligned} \tag{134}$$

and

$$\begin{aligned} V_4 = {} & H^+H^-\left(\lambda_2 H^+H^- + \frac{\lambda_3}{2}S_1^2 + \lambda_2 S_3^2 + \lambda_2 S_2^2 - \lambda_7^I S_1 S_3 + \lambda_7^R S_1 S_2\right) \\ & + \frac{1}{4}(\lambda_3 + \lambda_4 + 2\lambda_5^R)(S_1S_2)^2 + \frac{1}{4}(\lambda_3 + \lambda_4 - 2\lambda_5^R)(S_1S_3)^2 + \frac{\lambda_2}{2}(S_2S_3)^2 \\ & - \frac{1}{2}\lambda_6^I S_1^3 S_3 - \lambda_5^I S_1^2 S_2 S_3 - \frac{\lambda_7^I}{2}S_1 S_2^2 S_3 - \frac{\lambda_7^I}{2}S_1 S_3^3 + \frac{\lambda_6^R}{2}S_1^3 S_2 + \frac{\lambda_7^R}{2}S_1 S_2^3 + \frac{\lambda_7^R}{2}S_1 S_2 S_3^2 \\ & + \frac{\lambda_1}{4}S_1^4 + \frac{\lambda_2}{4}S_2^4 + \frac{\lambda_2}{4}S_3^4\,. \end{aligned} \tag{135}$$

5.2 Gauge sector

Once we have performed the symmetry breaking, interaction terms between the scalar fields, S_i and $H^\pm$, the Goldstone fields $G^\pm$ and G^0 and the gauge bosons $W_\mu^\pm, Z_\mu, A_\mu$ will arise. These terms will come from the covariant derivative, $D_\mu = \partial_\mu + ieQA_\mu + i\frac{g}{\cos\theta_{\rm w}}Z_\mu(T_3 - Q\sin^2\theta_{\rm w}) + ig[T_+W_\mu^\dagger + T_-W_\mu]$. In addition, we will have a term introduced to fix the gauge and cancel the quadratic mixing terms between the gauge and the Goldstone bosons,

$$\mathcal{L}_{\rm kin} + \sum_{i=1}^{2} D_\mu\Phi_a^\dagger D^\mu\Phi_a + \mathcal{L}_{GF} = \mathcal{L}_{V^2} + \mathcal{L}_{\phi^2} + \mathcal{L}_{\phi V} + \mathcal{L}_{\phi^2 V} + \mathcal{L}_{\phi V^2} + \mathcal{L}_{\phi^2 V^2}\,, \tag{136}$$

with the particular choice of the gauge-fixing term R_ε ($\varepsilon = 1$):

$$\mathcal{L}_{\rm GF} = -\frac{1}{2}(\partial_\mu A^\mu)^2 - \frac{1}{2}(\partial_\mu Z^\mu + M_Z G^0)^2 - (\partial^\mu W_\mu^\dagger + iM_W G^+)(\partial_\nu W^\nu - iM_W G^-)\,. \tag{137}$$

This gauge also provides the Goldstone bosons with the masses $M_{G^\pm} = M_W = gv/2$ and $M_{G^0} = M_Z = M_W/\cos\theta_{\rm w}$. Then,

$$\mathcal{L}_{V^2} = -\frac{1}{2}(\partial_\mu A^\mu)^2 - \frac{1}{2}(\partial_\mu Z^\mu)^2 + \frac{1}{2}M_Z^2 Z_\mu Z^\mu - (\partial^\mu W_\mu^\dagger)(\partial_\nu W^\nu) + M_W^2 W_\mu^\dagger W^\mu\,, \tag{138}$$

$$\begin{aligned}\mathcal{L}_{\phi^2} &= \frac{1}{2}[\partial_\mu h \partial^\mu h + \partial_\mu H \partial^\mu H + \partial_\mu A \partial^\mu A] + \partial_\mu H^+ \partial^\mu H^- \\ &+ \frac{1}{2}\partial_\mu G^0 \partial^\mu G^0 - \frac{1}{2} M_Z^2 (G_0)^2 + \partial_\mu G^+ \partial^\mu G^- - M_W^2 G^+ G^-\end{aligned} \tag{139}$$

$$\begin{aligned}\mathcal{L}_{\phi^2 V} =&\ ie[\,A^\mu + \cot(2\theta_\mathrm{w}) Z^\mu]\left[(H^+ \overset{\leftrightarrow}{\partial}_\mu H^-) + (G^+ \overset{\leftrightarrow}{\partial}_\mu G^-)\right] \\ &+ \frac{e}{\sin(2\theta_\mathrm{w})} Z^\mu \left[(G^0 \overset{\leftrightarrow}{\partial}_\mu S_1) + (S_3 \overset{\leftrightarrow}{\partial}_\mu S_2)\right] \\ &+ \frac{g}{2} W^{\mu\dagger}\left[(H^- \overset{\leftrightarrow}{\partial}_\mu S_3) - i(H^- \overset{\leftrightarrow}{\partial}_\mu S_2) + (G^- \overset{\leftrightarrow}{\partial}_\mu G^0) - i(G^- \overset{\leftrightarrow}{\partial}_\mu S_1)\right] \\ &+ \frac{g}{2} W^{\mu}\left[(H^+ \overset{\leftrightarrow}{\partial}_\mu S_3) + i(H^+ \overset{\leftrightarrow}{\partial}_\mu S_2) + (G^+ \overset{\leftrightarrow}{\partial}_\mu G^0) + i(G^+ \overset{\leftrightarrow}{\partial}_\mu S_1)\right],\end{aligned} \tag{140}$$

$$\begin{aligned}\mathcal{L}_{\phi V^2} &= \frac{2}{v} S_1 \left[\frac{1}{2} M_Z^2 Z_\mu Z^\mu + M_W^2 W_\mu^\dagger W^\mu\right] \\ &+ (e M_W A^\mu - g M_Z \sin^2\theta_\mathrm{w} Z^\mu)(G^+ W_\mu + G^- W_\mu^+)\,,\end{aligned} \tag{141}$$

$$\begin{aligned}\mathcal{L}_{\phi^2 V^2} =&\ \frac{1}{v^2}\left[\frac{1}{2} M_Z^2 Z_\mu Z^\mu + M_W^2 W_\mu^\dagger W^\mu\right][H^2 + h^2 + A^2 + (G^0)^2] \\ &+ \left\{e^2 [A^\mu + \cot(2\theta_\mathrm{w}) Z^\mu]^2 + \frac{g^2}{2} W_\mu^\dagger W^\mu\right\}(G^+ G^- + H^+ H^-) \\ &+ \frac{eg}{2}(A^\mu - \tan\theta_\mathrm{w} Z^\mu)[S_1(G^+ W_\mu + G^- W_\mu^\dagger) + S_2(H^+ W_\mu + H^- W_\mu) \\ &+ i S_3(H^- W_\mu^\dagger - H^+ W_\mu) + i G_0(G^- W_\mu^\dagger - G^+ W_\mu)]\,,\end{aligned} \tag{142}$$

with $A \overset{\leftrightarrow}{\partial}_\mu B \equiv A(\partial_\mu B) - (\partial_\mu A) B$.

As it can be seen in Eq. (141) the couplings are identical to the ones of the SM making the identification $H \leftrightarrow S_1$. This means

$$g^0_{\varphi_i VV} = \mathcal{R}_{i1} g^{SM}_{hVV}\,, \tag{143}$$

being VV = ZZ, WW. Which implies:

$$g^2_{hVV} + g^2_{HVV} + g^2_{AVV} = (g^{SM}_{hVV})^2\,. \tag{144}$$

This result indicates that the coupling to weak bosons cannot be enhanced over the SM value and must obey custodial symmetry, $g_{\varphi_i^0 ZZ} = g_{\varphi_i^0 WW}$.

5.3 Yukawa sector and the Aligned two-Higgs doublet model

The two doublets of our model have the same quantum numbers as the SM doublet, so the most generic form of the Yukawa Lagrangian will be very similar to the one in Eq. (75), containing extra terms related to the new doublet,

$$\mathcal{L}_Y = -\bar{\mathbf{Q}}'_L(\mathbf{\Gamma}_1 \phi_1 + \mathbf{\Gamma}_2 \phi_2)\mathbf{d}'_R - \bar{\mathbf{Q}}'_L(\mathbf{\Delta}_1 \tilde{\phi}_1 + \mathbf{\Delta}_2 \tilde{\phi}_2)\mathbf{u}'_R - \bar{\mathbf{L}}'_L(\mathbf{\Pi}_1 \phi_1 + \mathbf{\Pi}_2 \phi_2)\mathbf{l}'_R + \text{h.c.} \tag{145}$$

where, $\mathbf{\Gamma}_i$, $\mathbf{\Delta}_i$ and $\mathbf{\Pi}_i$ are $N_G \times N_G$ complex matrices in flavour space describing the coupling. Since we are working in the Higgs basis, it is convenient to express $\mathcal{L}_Y$ in terms of Φ_1 and Φ_2,

$$\mathcal{L}_Y = -\frac{\sqrt{2}}{v}\left\{\bar{\mathbf{Q}}'_L(\mathbf{M}'_d \Phi_1 + \mathbf{Y}'_d \Phi_2)\mathbf{d}'_R - \bar{\mathbf{Q}}'_L(\mathbf{M}'_u \tilde{\Phi}_1 + \mathbf{Y}'_u \tilde{\Phi}_2)\mathbf{u}'_R - \bar{\mathbf{L}}'_L(\mathbf{M}'_l \Phi_1 + \mathbf{Y}'_l \Phi_2)\mathbf{l}'_R + \text{h.c}\right\} \tag{146}$$

being $\mathbf{M}'_a$ the same non-diagonal mass matrices as in Eq. (75) of Section 3.4. As before, we can diagonalize these matrices by performing transformations in the fields, paying the price of introducing the

CKM matrix, but nothing guarantees us that the matrices $\mathbf{Y}_a$ will be diagonal. These non-diagonal matrices will introduce dangerous FCNC interactions, which are tightly constrained phenomenologically [17]. To avoid these FCNC effects several solutions can be proposed. Firstly, one can impose that the non-diagonal Yukawa matrices are proportional to the geometric mean of the fermion masses $\propto \sqrt{m_i m_j}$. This is known as Type III 2HDM, as can be seen in [18]. In others models, the scalars are so heavy that suppress the low energy FCNC effects, leading to a phenomenologically non-relevant 2HDM.

A more elegant solution that will be explored here is the known as A2HDM, in which we require that the Yukawa couplings $\mathbf{Y}_a$ are aligned in flavour space with the diagonal mass matrices,

$$\Gamma_2 = \varepsilon_d e^{-i\varepsilon}\Gamma_1\,, \qquad \Delta_2 = \varepsilon_u^* e^{i\varepsilon}\Delta_1\,, \qquad \Pi_2 = \varepsilon_l e^{-i\varepsilon}\Pi_1\,. \tag{147}$$

With that, once we express our Lagrangian in the Φ_i basis we have

$$\begin{aligned}
\mathbf{\Gamma}_1\phi_1 + \mathbf{\Gamma}_2\phi_2 =& \frac{\mathbf{\Gamma}_1}{v}\Big[\Phi_1(v_1+\varepsilon_d v_2) + \Phi_2(-v_2+\varepsilon_d v_1)\Big]\,, \\
\mathbf{\Delta}_1\tilde{\phi}_1 + \mathbf{\Delta}_2\tilde{\phi}_2 =& \frac{\mathbf{\Delta}_1}{v}\Big[\tilde{\Phi}_1(v_1+\varepsilon_u^* v_2) + \tilde{\Phi}_2(-v_2+\varepsilon_u^* v_1)\Big]\,, \\
\mathbf{\Pi}_1\phi_1 + \mathbf{\Pi}_2\phi_2 =& \frac{\mathbf{\Pi}_1}{v}\Big[\Phi_1(v_1+\varepsilon_l v_2) + \Phi_2(-v_2+\varepsilon_l v_1)\Big]\,.
\end{aligned} \tag{148}$$

From here we have

$$\begin{aligned}
\mathbf{M}'_d =& \frac{\mathbf{\Gamma}_1}{v}(v_1+\varepsilon_d v_2)\,, \qquad \mathbf{Y}'_d = \frac{\mathbf{\Gamma}_1}{v}(-v_2+\varepsilon_d v_1) = \varsigma_d \mathbf{M}'_d\,, \\
\mathbf{M}'_u =& \frac{\mathbf{\Delta}_1}{v}(v_1+\varepsilon_u^* v_2)\,, \qquad \mathbf{Y}'_u = \frac{\mathbf{\Delta}_1}{v}(-v_2+\varepsilon_u^* v_1) = \varsigma_u^* \mathbf{M}'_u\,, \\
\mathbf{M}'_l =& \frac{\mathbf{\Pi}_1}{v}(v_1+\varepsilon_l v_2)\,, \qquad \mathbf{Y}'_l = \frac{\mathbf{\Pi}_1}{v}(-v_2+\varepsilon_l v_1) = \varsigma_l \mathbf{M}'_l\,,
\end{aligned} \tag{149}$$

Thus, $\mathbf{M}'_i$ and $\mathbf{Y}'_i$ will be related by the function:

$$\varsigma_f = \frac{\varepsilon_i v_1 - v_2}{v_1 + \varepsilon_i v_2} = \frac{\varepsilon_i - \tan\beta}{1+\varepsilon_i\tan\beta}\,, \tag{150}$$

where $\tan\beta = \frac{v_2}{v_1}$.

As we did in the SM in Section 3.3 we can perform transformations in the fields to diagonalize the mass matrices, paying the cost of introducing the CKM matrix, V. In terms of the mass eigenstates, the Yukawa Lagrangian takes the form:

$$\mathcal{L}_Y = -\frac{\sqrt{2}}{v}H^+\Big\{\bar{u}(x)[\varsigma_d V\mathbf{M}_d\mathcal{P}_R - \varsigma_u\mathbf{M}_u^\dagger V\mathcal{P}_L]d(x) + \varsigma_l\bar{\nu}(x)\mathbf{M}_l\mathcal{P}_R l(x)\Big\} \tag{151}$$

$$-\frac{1}{v}\sum_{\varphi_i^0, f} y_f^{\varphi_i^0}\varphi_i^0[\bar{f}(x)\mathbf{M}_f\mathcal{P}_R f(x)] + \text{h.c.}\,. \tag{152}$$

$\mathcal{P}_{L,R}$ are the quirality projectors and $y_f^{\varphi_i^0}$ are the neutral couplings for the physical scalar fields, given by:

$$y_{d,l}^{\varphi_i^0} = \mathcal{R}_{i1} + (\mathcal{R}_{i2} + i\mathcal{R}_{i3})\varsigma_{d,l}\,, \qquad y_u^{\varphi_i^0} = \mathcal{R}_{i1} + (\mathcal{R}_{i2} - i\mathcal{R}_{i3})\varsigma_u^*\,. \tag{153}$$

The consequences of the alignment are interesting. Firstly, all scalar-fermion couplings are proportional to the fermion masses, and the neutral Yukawas are diagonal in flavour. As in the SM, in the A2HDM there are no right-handed neutrinos, so all the leptonic couplings are diagonal in flavour, having as a consequence the lack of lepton-flavour-violating neutral couplings in all orders in perturbation theory. Regarding to the flavour-changing interactions, the only possible contribution to them is the CKM matrix in the charged sector.

Model	ς_d	ς_u	ς_l
Type I	$\cot\beta$	$\cot\beta$	$\cot\beta$
Type II	$-\tan\beta$	$\cot\beta$	$-\tan\beta$
Type X	$\cot\beta$	$\cot\beta$	$-\tan\beta$
Type Y	$-\tan\beta$	$\cot\beta$	$\cot\beta$
Inert	0	0	0

Table 1: CP-conserving 2HDMs based on discrete $\mathcal{Z}_2$ symmetries, being $\tan\beta \equiv v_2/v_1$

There are only three new parameters ς_f, which encode all the possible freedom in the alignment. These couplings satisfy universality among generations, are invariant under global $SU(2)$ transformations of scalar fields, $\phi_a \to \phi'_a = U_{ab}\phi_b$ and since, in general, are complex numbers, their phases introduce new sources of CP violation. The usual models with natural flavour conservation, based on discrete symmetries, $\mathcal{Z}_2$, are recovered for particular real values of ς_f as it can be seen in Table 1.

From the orthogonality of the rotation matrix, $\mathcal{R}$ we can also obtain the relations [19],

$$\sum_{i=1}^{3}(y_f^{\varphi_i^0})^2 = 1\,, \quad \sum_{i=1}^{3}|y_f^{\varphi_i^0}|^2 = 1 + 2|\varsigma_f|^2\,, \quad \sum_{i=1}^{3} y_f^{\varphi_i^0}\mathcal{R}_{i1} = 1\,, \tag{154}$$
$$\sum_{i=1}^{3} y_{d,l}^{\varphi_i^0}\mathcal{R}_{i2} = \varsigma_{d,l}\,, \qquad \sum_{i=1}^{3} y_u^{\varphi_i^0}\mathcal{R}_{i2} = \varsigma_u^*\,,$$
$$\sum_{i=1}^{3} y_{d,l}^{\varphi_i^0}\mathcal{R}_{i3} = i\varsigma_{d,l}\,, \qquad \sum_{i=1}^{3} y_u^{\varphi_i^0}\mathcal{R}_{i3} = -i\varsigma_u^*\,.$$

5.4 Phenomenology and Higgs signal strengths

The A2HDM has a richer phenomenology than the SM. First of all, since the Higgs-like particles are a mixture of the two CP-even scalars, $S_{1,2}$ and the CP-odd scalar, S_3, the processes involving φ_i^0 will have contributions from both even and odd particles. In the CP-conserving limit the mixture between CP-even and CP-odd particles disappears, so two of the Higgs-like particles will be CP-even and their couplings to fermions and neutral bosons will be the same as in the SM, with different constant factors as we have seen in Eq. (143) and (153). In addition, we will have new vertices corresponding to the CP-odd Higgs boson that were not present in the SM.

In this limit, the couplings of the A2HDM with respect to the SM ones for fermions, take the form:

$$y_f^h = \cos\tilde{\alpha} + \varsigma_f \sin\tilde{\alpha}\,, \qquad y_{d,l}^A = i\varsigma_{d,l}\,, \tag{155}$$
$$y_f^H = -\sin\tilde{\alpha} + \varsigma_f \cos\tilde{\alpha}\,, \qquad y_u^A = -i\varsigma_u\,.$$

And, for weak bosons, with $\kappa_V^{\varphi_i^0}$ defined as $\kappa_V^{\varphi_i^0} \equiv g_{\varphi_i^0 VV}/g_{HVV}^{SM}$.

$$\kappa_V^h = \cos\tilde{\alpha}\,, \qquad \kappa_V^H = -\sin\tilde{\alpha}\,, \qquad \kappa_V^A = 0\,, \tag{156}$$

which means that in this limit only the CP-even Higgs-like particles, h and H, couple to weak bosons. This implies that the decay of A into weak bosons cannot exist at tree level, and therefore it will be very suppressed.

Having fixed the gauge as we did in Section 5.2, besides the Higgs-like particles, the only new particles of our model are the charged scalars, $H^\pm$, which couple to bosons. In this section, we will describe these new ingredients, absent in the SM, and we will compare with the experimental data of current colliders.

The relevant processes within the model will be described, focusing on the differences with respect to the SM. Then, we will write the Higgs signal strengths, as described in Appendix A, and finally we will perform a χ^2 minimization, as we did in Sections 4.2.1 and 4.2.2.

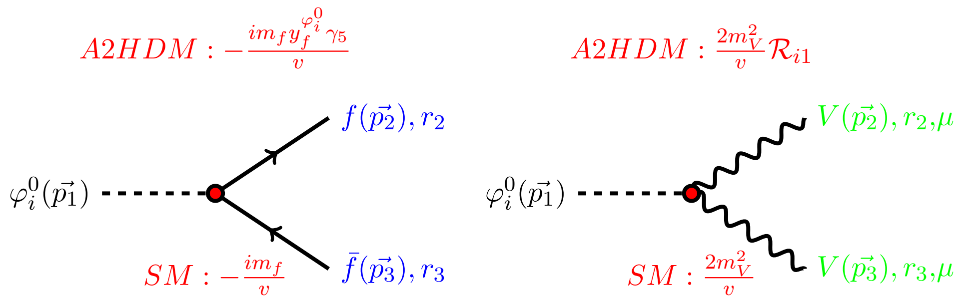

Figure 12: Higgs coupling to fermions (left) and to weak bosons (right) both in the SM and in the A2HDM.

To calculate the strengths of the relevant processes, as expressed in Section A and perform a χ^2 test, let's remind the general form of the Higgs signal strength:

$$\mu_X^{\varphi_i^0} = \frac{\sigma(pp \to \varphi_i^0)\mathrm{BR}(\varphi_i^0 \to X)}{\sigma(pp \to h)_{SM}\mathrm{BR}(h \to X)_{SM}}\,, \qquad \mu_{Xjj}^{\varphi_i^0} = \frac{\sigma(pp \to jj\varphi_i^0) \quad \mathrm{BR}(\varphi_i^0 \to X)}{\sigma(pp \to jjh)_{SM}\mathrm{BR}(h \to X)_{SM}}\,, \tag{157}$$

being X the possible final states studied, i.e, $X = \gamma\gamma, WW, ZZ, \tau^+\tau^-, bb$.

The ratio of the A2HDM and SM branching ratios is given by:

$$\frac{\mathrm{BR}(\varphi_i^0 \to X)}{\mathrm{BR}(h \to X)_{SM}} = \frac{\Gamma(\varphi_i^0 \to X)}{\Gamma(\varphi_i^0)}\frac{\Gamma(h)_{SM}}{\Gamma(h \to X)_{SM}} = \frac{1}{\rho(\varphi_i^0)}\frac{\Gamma(\varphi_i^0 \to X)}{\Gamma(h \to X)_{SM}}\,, \tag{158}$$

with

$$\rho(\varphi_i^0) = \frac{\Gamma_{\varphi_i^0}}{\Gamma_{SM}(h)}\,. \tag{159}$$

Assuming only one dominant production channel and taking into account that the ratios are defined for $M_{\varphi_i^0} = M_{h_{SM}}$ we find for the general case:

$$\begin{aligned}
\mu_{bb}^{\varphi_i^0} &= C_{gg}^{\varphi_i^0}\left[\mathrm{Re}(y_d^{\varphi_i^0})^2 + \mathrm{Im}(y_d^{\varphi_i^0})^2\beta_b^{-2}\right]\rho(\varphi_i^0)^{-1}, & \mu_{\gamma\gamma}^{\varphi_i^0} &= C_{gg}^{\varphi_i^0}C_{\gamma\gamma}^{\varphi_i^0}\rho(\varphi_i^0)^{-1}\,,\\
\mu_{\tau\tau}^{\varphi_i^0} &= C_{gg}^{\varphi_i^0}\left[\mathrm{Re}(y_l^{\varphi_i^0})^2 + \mathrm{Im}(y_l^{\varphi_i^0})^2\beta_\tau^{-2}\right]\rho(\varphi_i^0)^{-1}, & \mu_{\gamma\gamma jj}^{\varphi_i^0} &= (\mathcal{R}_{i1})^2C_{\gamma\gamma}^{\varphi_i^0}\rho(\varphi_i^0)^{-1}\,,\\
\mu_{bbV}^{\varphi_i^0} &= (\mathcal{R}_{i1})^2\left[\mathrm{Re}(y_d^{\varphi_i^0})^2 + \mathrm{Im}(y_d^{\varphi_i^0})^2\beta_b^{-2}\right]\rho(\varphi_i^0)^{-1}, & \mu_{VV}^{\varphi_i^0} &= C_{gg}^{\varphi_i^0}(\mathcal{R}_{i1})^2\rho(\varphi_i^0)^{-1}\,,\\
\mu_{\tau\tau V}^{\varphi_i^0} &= (\mathcal{R}_{i1})^2\left[\mathrm{Re}(y_l^{\varphi_i^0})^2 + \mathrm{Im}(y_l^{\varphi_i^0})^2\beta_\tau^{-2}\right]\rho(\varphi_i^0)^{-1}\,, & \mu_{VVjj}^{\varphi_i^0} &= (\mathcal{R}_{i1})^4\rho(\varphi_i^0)^{-1}\,,
\end{aligned} \tag{160}$$

where $\beta_f = (1 - 4m_f^2/M_{\varphi_i^0}^2)^{1/2}$.

It is important to note that the strengths containing two separated terms as $\mu_{bb(V)}^{\varphi_i^0}$ and $\mu_{\tau\tau(V)}^{\varphi_i^0}$ are related to the CP-even scalars, $S_{1,2}$, (real parts) and to the CP-odd scalar, S_3, (imaginary parts), with fermionic couplings given in the left panel Fig. 12. The factors $\mathcal{R}_{i1}$ are due to the ratio between the SM and the A2HDM coupling in the case of weak bosons, as it can be seen in the right panel of Fig. 12. Detailed calculation of the decay widths and cross sections that appear in the strengths can be seen in Appendix B.

$C_{gg}^{\varphi_i^0}$ and $C_{\gamma\gamma}^{\varphi_i^0}$ are the one-loop functions, given by:

$$C_{gg}^{\varphi_i^0} = \frac{\sigma(gg \to \varphi_i^0)}{\sigma(gg \to h)_{SM}} = \frac{|\sum_q \mathrm{Re}(y_q^{\varphi_i^0})\mathcal{F}(x_q)|^2 + |\sum_q \mathrm{Im}(y_q^{\varphi_i^0})\mathcal{K}(x_q)|^2}{|\sum_q \mathcal{F}(x_q)|^2} \tag{161}$$

and

$$C_{\gamma\gamma}^{\varphi_i^0} = \frac{\Gamma(\varphi_i^0 \to \gamma\gamma)}{\Gamma(h \to \gamma\gamma)_{SM}} = \frac{|\sum_q \mathrm{Re}(y_f^{\varphi_i^0})N_C^fQ_f^2\mathcal{F}(x_f) + \mathcal{G}(x_w)\mathcal{R}_{i1} + \mathcal{C}_{H^\pm}^{\varphi_i^0}|^2 + |\sum_f \mathrm{Im}(y_f^{\varphi_i^0})N_C^fQ_f^2\mathcal{K}(x_f)|^2}{|\sum_f N_C^fQ_f^2\mathcal{F}(x_f) + \mathcal{G}(x_w)|^2}\,, \tag{162}$$

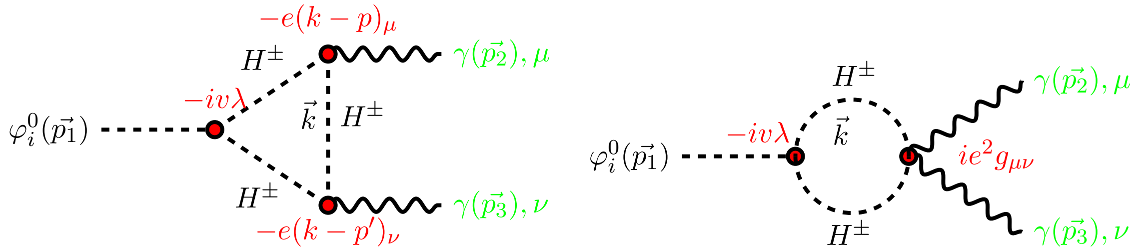

Figure 13: Loops with the scalar particle, $H^\pm$ contributing to the process $\varphi_i^0 \to \gamma\gamma$.

where, again, the real and imaginary terms correspond to the CP-even and to the CP-odd particles respectively. N_C^f and Q_f are the colour number and the electric charge of the fermions, $x_f = 4m_f^2/M_{\varphi_i^0}^2$ and $x_W = 4M_W^2/M_{\varphi_i^0}^2$. The term $\mathcal{C}_{H^\pm}^{\varphi_i^0}$ in the photon loop is a new contribution of the A2HDM, given in Fig. 13 and which takes the form:

$$\mathcal{C}_{H^\pm}^{\varphi_i^0} = \frac{v^2}{2M_{H_\pm}^2}\lambda_{\varphi_i^0 H^+H^-}\mathcal{A}(x_{H_\pm})\,. \tag{163}$$

being $\lambda_{\varphi_i^0 H^+H^-}$ the cubic coupling between the Higgs-like boson φ_i^0 and the charged Higgs, which can be related to the parameters of the potential, as it can be seen in Eq. (134). If CP is assumed to be an exact symmetry, $\lambda_{AH^+H^-} = 0$.

The explicit expressions of the loop functions are:

$$\begin{aligned} \mathcal{F}(x) &= \frac{x}{2}[4+(x-1)f(x)]\,, & \mathcal{G}(x) &= -2-3x+\left(\frac{3}{2}x-\frac{3}{4}x^2\right)f(x)\,, \\ \mathcal{A}(x) &= -x-\frac{x^2}{4}f(x)\,, & \mathcal{K}(x) &= -\frac{x}{2}f(x)\,, \end{aligned} \tag{164}$$

with

$$f(x) = \begin{cases} -4\arcsin^2(1/\sqrt{x}), & x \geq 1 \\ \left[\ln\left(\frac{1+\sqrt{1-x}}{1-\sqrt{1-x}}\right) - i\pi\right]^2, & x < 1\,. \end{cases} \tag{165}$$

5.5 Global fits for the A2HDM in the CP-conserving limit

As it is indicated in Eq. (155) and (156) if our Lagrangian preserves the CP symmetry the CP-even scalars h and H couple to gauge bosons with reduced couplings $\mathcal{R}_{11}$ and $\mathcal{R}_{21}$ and their Yukawa couplings are real, while the CP-odd scalar does not couple to weak bosons and their Yukawa couplings are purely imaginary [19].

In this section, in order to obtain values for the parameters of the theory, a χ^2 minimization will be performed in the context of the CP-conserving limit. Details about the statistics are given in Appendix A.

First, in Sections 5.5.1 and 5.5.2 we will analyze the possibility in which the lightest scalar corresponds to the observed Higgs, h, with a mass, $M_h = 125$ GeV, both not including and including the charged scalar loop $H^\pm$ of Fig. 13. Later in Section 5.5.3 the possibility of the observed Higgs to be the CP-odd Higgs will be analyzed. Similar analyses can be found in [19, 20].

5.5.1 Light CP-even Higgs at 125 GeV without $H^\pm$ loop

In our first analysis we assume that the loop of charged scalars, $H^\pm$, does not contribute to the diphoton decay, i.e, $\mathcal{C}_{H^\pm}^h \approx 0$, which means either $H^\pm$ is very heavy, or the coupling is very small. In the next section, the case in which this process is not omitted will be studied.

The minimization of the χ^2 function give us the following values for the relevant parameters and their 1σ uncertainties. Looking at the form of the χ^2 function we can see that for the Yukawa couplings,

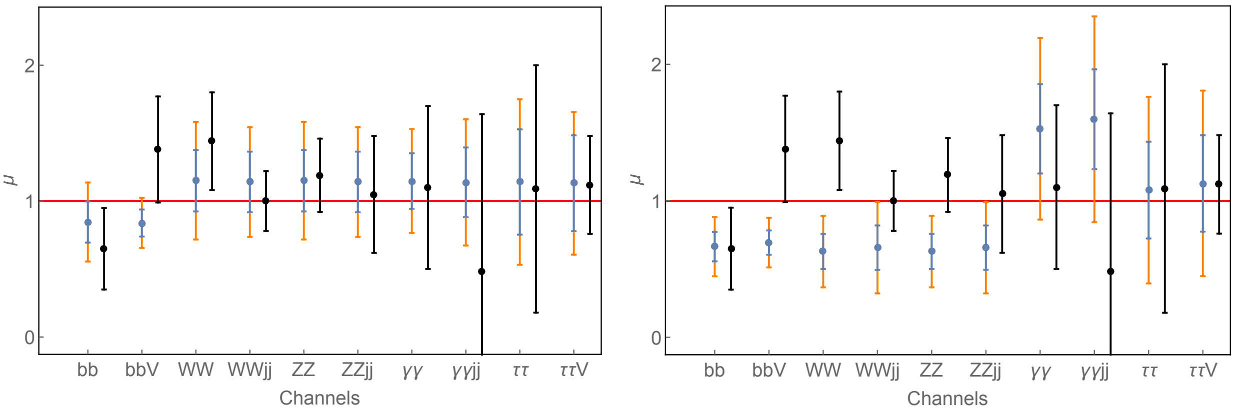

Figure 14: Higgs signal strengths for the CP-even light Higgs without the $H^\pm$ loop with a positive value of y_u^h (left panel) and a negative value (right panel). In blue and orange we have the results for the fit at 1σ and 2σ respectively. In black we have the experimental data with an uncertainty of 1σ.

y_d^h and y_l^h the only information we can get from the fit is their absolute values. The minimization give us two different sets of parameters, depending on the relative sign between y_u^h and $\cos\tilde{\alpha}$,

$$\cos\tilde{\alpha} = 0.98^{+0.02}_{-0.06}\,, \quad y_u^h = 0.98 \pm 0.08\,, \quad |y_d^h| = 0.84^{+0.08}_{-0.09}\,, \quad |y_l^h| = 0.97^{+0.14}_{-0.16}\,, \tag{166}$$

and $\chi^2/\text{d.o.f} = 0.47$.

$$\cos\tilde{\alpha} = 0.83 \pm 0.06\,, \quad y_u^h = -0.83 \pm 0.06\,, \quad |y_d^h| = 0.87^{+0.08}_{-0.09}\,, \quad |y_l^h| = 1.12^{+0.15}_{-0.18}\,, \tag{167}$$

and $\chi^2/\text{d.o.f} = 2.96$.

In the first solution, the relative sign between y_u^h and $\cos\tilde{\alpha}$ is positive, which means that the quark loop (in which the top loop dominates) and the $W^\pm$ contribute with different signs, giving a destructive interference as in the SM.[14] This gives a ratio between the decay widths of $\rho(h) = 0.80^{+0.11}_{-0.14}$ and the strengths of the left panel of Fig. 14, from where it can be seen that all the channels are compatible with the experimental results at 1σ.

The second, solution corresponding to $y_u^h < 0$ and $\cos\tilde{\alpha} > 0$ gives a much worse fit as we can see from the value of the χ^2 / d.o.f. In this case the top-quark loop contribution and the W-boson interfere constructively, which makes it more difficult to reproduce the $\gamma\gamma$ signal without adding new ingredients (as the $H^\pm$ loops). For this fit we find $\rho(h) = 0.77^{+0.14}_{-0.11}$. In the right panel of Fig. 14 the signal strengths for this case can be seen, resulting in a worse agreement that for the previous fit.

In Fig. 15 the allowed regions of $y_u^h - y_d^h$ (left) and $y_u^h - y_l^h$ (right) are shown graphically at 86% (1σ), 90% and 99% CL. The rest of the parameters are fixed to the central values of the fit. From here it can be seen the degeneracy in the sign of y_d^h and y_l^h, as well as the difference in the results for $y_u^h > 0$ and $y_u^h < 0$.

5.5.2 Light CP-even Higgs at 125 GeV with $H^\pm$ loop

As it has been previously mentioned, a new ingredient of the A2HDM with respect to the SM is the presence of a charged scalar particle, $H^\pm$, that couples to the scalars, S_i, as well as to weak bosons and photons, as it can be seen in Eq. (134) - (141). This introduces a modification in $C_{\gamma\gamma}^{\varphi_i^0}$.

The current and less restrictive lower bound for the $H^\pm$ mass is 72.5 GeV, obtained assuming a type-I fermionic structure and allowing the decay $H^\pm \to W^\pm A \to W^\pm b\bar{b}$ as well as the fermionic decays [21]. A model independent bound can be extracted from the masured Z width, to $M_{H^\pm} \gtrsim 39.6$ GeV at a 95% confidence level (CL) [21].

As we have seen in Eq. (162) the $H^\pm$ loop can interfere with the $W^\pm$ and fermionic loops. By the perturbative arguments given in Appendix C we expect $|\mathcal{C}^h_{H^\pm}| \lesssim \mathcal{O}(10^1)$ GeV, which will be translated into an allowed region for the values of $\lambda_{hH^+H^-}$ and $M_{H^\pm}$.

[14] Note that $\mathcal{F}(x_t) > 0$, while $\mathcal{G}(x_W) < 0$.

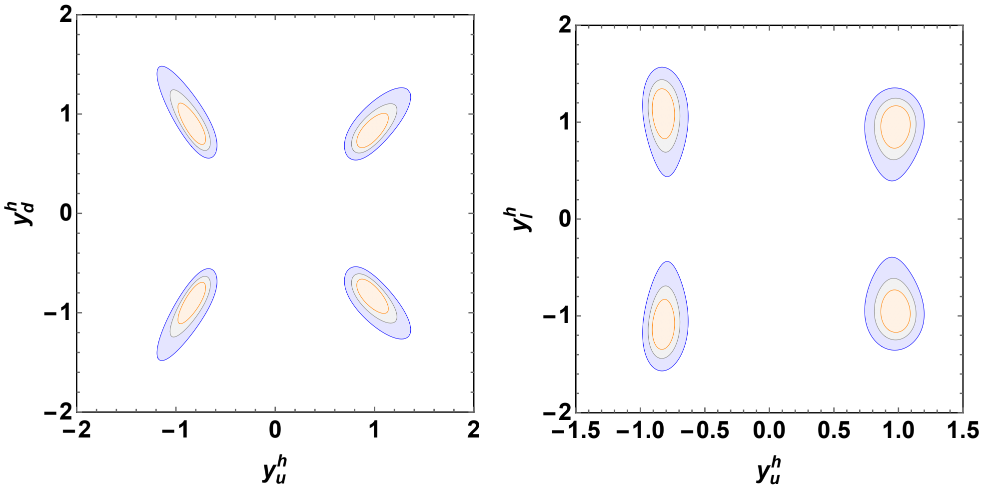

Figure 15: Global fit for an even scalar of the A2HDM model in the CP-conserving limit and ignoring the contribution of the $H^{\pm}$ loop, in the planes $y_u^h - y_d^h$ (left) and $y_u^h - y_l^h$ (right). The orange, gray and blue regions represent 68%, 90% and 99% CL regions.

Including this new parameter in our fit and with the signs of y_u and $\cos\tilde{\alpha}$ taken as in the SM we obtain a $\chi^2/$ d.o.f. of 0.59 with:

$$\begin{aligned} \cos\tilde{\alpha} = 0.98^{+0.02}_{-0.05}\,, \qquad \mathcal{C}^h_{H^{\pm}} = (-0.03^{+0.70}_{-0.61} \cup 12.68^{+0.70}_{-0.67})\,, \\ y_u^h = 0.98 \pm 0.08\,, \quad |y_d^h| = 0.84^{+0.08}_{-0.09}\,, \quad |y_l^h| = 0.97^{+0.14}_{-0.16}\,. \end{aligned} \tag{168}$$

The two disjoint solutions of $\mathcal{C}^h_{H^{\pm}}$ reverse the sign of the argument of $C^h_{\gamma\gamma}$, so its absolute value is the same, corresponding to a destructive interference ($\mathcal{C}^h_{H^{\pm}} > 0$) or to a constructive one ($\mathcal{C}^h_{H^{\pm}} < 0$). In both cases the fit is better than the one of Eq. (167) and comparable to (166). The total decay with is modified to $\rho = 0.80^{+0.11}_{-0.12}$ similarly to the case of (166).

In Fig. 16 (left) the Higgs signal strengths of the fit are compared with the experimental ones, at one and two σ CL, showing a good agreement with the experimental data. The allowed regions of $y_u^h - y_d^h$ (left) and $y_u^h - y_l^h$ (right) are shown in Fig. 17 for a 68%, 90% and 99% CL.

In the right panel of Fig. 16 the allowed regions for the $(|\lambda_{hH^+H^-}|, M_{H^{\pm}})$ are shown, corresponding to the two possible values fitted for $\mathcal{C}^h_{H^{\pm}}$ at 1σ CL, together with the perturbative bounds, as discussed in Appendix C. The solution with a larger contribution from the charged Higgs is excluded by perturbative arguments.

5.5.3 CP-odd Higgs at 125 GeV

To finish with our analysis for the CP-conserving limit we should study the possibility of the observed Higgs to be the CP-odd particle, A. In this case the fit gives us a worse result than in the previous cases. This is because, as it can be seen from Eq. (141) a CP-odd boson does not couple to weak bosons at tree level, so these decays are very suppressed, and consequently some of the Higgs signal strengths considered at (160) will be zero. [15]

Performing the χ^2 minimization as in the previous sections we find $\chi^2/\text{d.o.f.} = 11.6$ with the following values:

$$|y_u^A| = 0.84 \pm 0.07\,, \quad |y_d^A| = 0.34^{+0.10}_{-0.08}\,, \quad |y_l^h| = 0.35^{+0.09}_{-0.12}\,. \tag{169}$$

Having such a large value for $\chi^2/\text{d.o.f.}$ indicates us that we are on a more unlikely case than previously. The study of the Higgs strengths and of the total decay width also indicate us that this possibility is very disfavoured by the present data.

[15] As it can be easily seen since $\mathcal{R}_{13} = 0$.

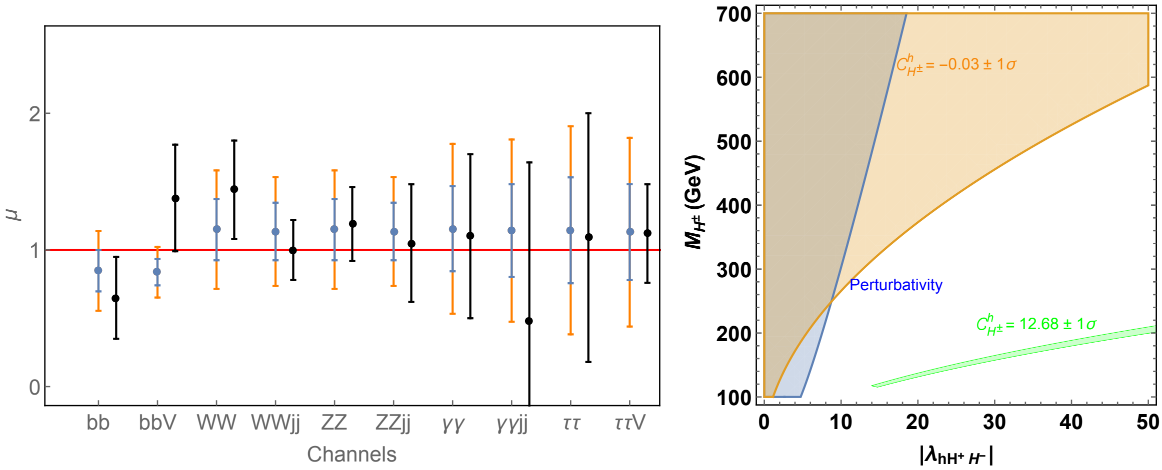

Figure 16: **Left:** Higgs signal strengths for the CP-even light Higgs considering the loop of charged $H^{\pm}$. In blue and orange we have the results for the fit at 1σ and 2σ respectively. In black we have the experimental data with an uncertainty of 1σ. **Right:** Allowed regions for $(|\lambda_{hH^+H^-}|, M_{H^\pm})$ plane, corresponding to the two possible fitted values of $\mathcal{C}^h_{H^\pm}$ at 1σ CL. The blue region shows the values for $(|\lambda_{hH^+H^-}|, M_{H^\pm})$ for which $\mathcal{C}^h_{H^\pm}$ is perturbative.

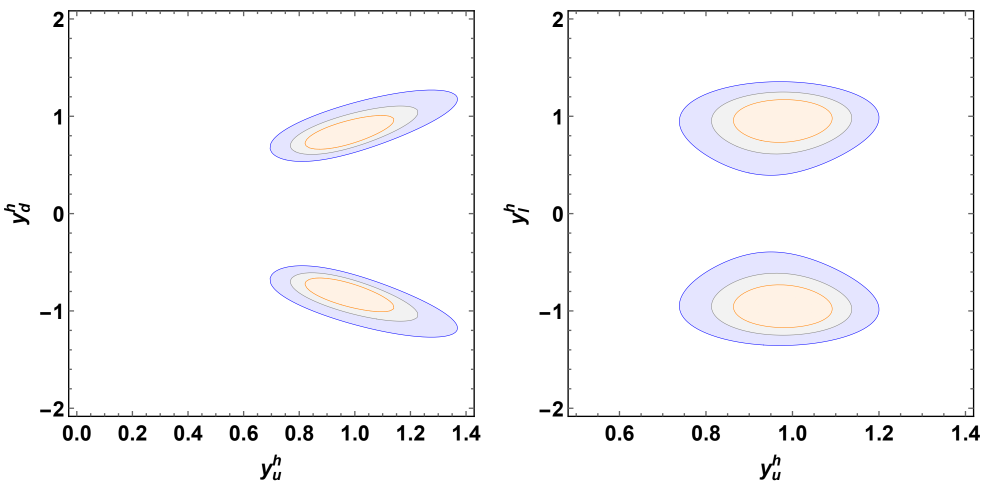

Figure 17: Global fit for an even scalar of the A2HDM model in the CP-conserving limit taking into account the contribution of the $H^{\pm}$ loop, in the planes $y^h_u - y^h_d$ (left) and $y^h_u - y^h_l$ (right). The orange, gray and blue regions represent 68%, 90% and 99% CL regions.

6 Diphoton excess

Both ATLAS and CMS collaborations have recently presented the first preliminary results obtained at the LCH Run 2, with pp collision at a center of mass energy of $\sqrt{s} = 13$ TeV. An excess of diphoton signal has been observed, corresponding to a resonance of an invariant mass around 750 GeV.

The ATLAS collaboration [22] has 3.2 fb^{-1} of data and claims a local significance of 3.9σ, corresponding to 14 events excess, and 2.3σ of global signifance in the Large Width (LW) fit.[16] This result is compatible with the CMS data [23], which employs 2.6fb^{-1} of data and has observed an excess of 10 events with a local significance of 2.6σ and global significance of 1.2σ in the LW fit and 2σ in the Narrow Width (NW) fit. In addition, the CMS collaboration presented the combined results that include 19.7fb^{-1} data of the Run 1 ($\sqrt{s} = 8$ TeV), which exhibits an excess at the same energy and enhances the local significance to 3.1σ [24, 25]. Not combined data is presented for ATLAS, since its Run 1 extends only to 600 GeV.

The most simple interpretation of this, is to consider the excess as the resonant process $pp \to S \to \gamma\gamma$, where S is a new uncolored boson with mass around 750 GeV, and given that spin-1 decays into photons are forbidden by the Landau-Yang theorem, the particle S will have either spin zero or two. Further, if this new particle is neutral, its coupling to photons has to be mediated by a loop of charged particles. As we will see in the following it would be necessary to add such charged particles to reproduce the diphoton signal. Properties and quantum numbers of these new charged particles can be constrained by studying the decays of S, as it is done in [26].

In this section we will study the significance of this signal on the scalar extensions of the SM studied in Section 4 and Section 5 using the data of our χ^2 fit and considering both the possibility of a NW or a LW fit. To perform such analysis we will assume an invariant mass spectrum of 750 GeV, suggesting a cross section times branching ratio for the $8 + 13$ TeV CMS data of

$$\sigma^{CMS}_{pp\to S}\mathrm{BR}^{CMS}_{S\to\gamma\gamma} = 4.47 \pm 1.86 \text{ fb}\,. \tag{170}$$

obtained by the combination of 8 and 13 TeV data, properly scaled with the kinematic factors needed to convert a cross section at 8 TeV into a effective one at 13 TeV.

For ATLAS the most significant excess is observed around 747 GeV at 13 TeV

$$\sigma^{ATLAS}_{pp\to S}\mathrm{BR}^{ATLAS}_{S\to\gamma\gamma} = 10.6 \pm 2.9 \text{ fb}\,. \tag{171}$$

Using both results we have a combined cross section times branching ratio of

$$\hat{\sigma}_{pp\to S}\widehat{\mathrm{BR}}_{S\to\gamma\gamma} = 6.26 \pm 3.32 \text{ fb}\,. \tag{172}$$

To see if our models can reproduce the experimental excess we will consider the quantity $\sigma_{pp\to S}BR_{S\to\gamma\gamma}$ together with the values of the total cross section of the LW and the NW fit.

6.1 Diphoton excess in the singlet model

As we are about to see the singlet model explained in Section 4 cannot accommodate the diphoton excess without adding any new ingredient. In this model the $\gamma\gamma$ decay can only be suppressed by a factor $\cos\theta$ or $\sin\theta$ with respect to the SM value, as we will see in the following sections. We will use the data obtained from our global fits of Section 4.

In both cases the values of $\sigma(pp \to h_i)$ and $\Gamma(h_i \to \gamma\gamma)$ are fixed by the values of $\cos\theta$ and $\sin\theta$ obtained from the minimization of the χ^2 function. In the case of the heavy scenario the total decay width of the Higgs-like particle, h_1 can also have contributions from the decay $h_1 \to h_2h_2$ with the unknown parameter $\widetilde{\mu}$ as defined in Eq. (109).

[16] Here, we will refer both to a Large Width fit (LW) and to a Narrow fit (NW). We note, that for LW $\Gamma \approx 45$ GeV, while for NW $\Gamma \approx 0.1$ GeV [26].

6.1.1 Heavy scenario

First of all, let's look at the total width of the heavy Higgs, h_1. Using the value for the $\cos\theta$ of Section 4 we get $\cos\theta = 0.14 \pm 0.07$ which yields into a total width of

$$\Gamma_{h_1} = 12.7 + \Gamma_{h_1 \to h_2 h_2} \pm 12.6 \text{ GeV}\,. \tag{173}$$

where $\Gamma_{h_1 \to h_2 h_2}$ is the possible decay of h_1 into two lighter Higgs-like scalars and 12.7 ± 12.6 GeV is the decay width of h_1 into the observable channels obtained using the value for the $\cos\theta$. Here, we have also included the kinematically forbidden decays for the 125 GeV boson, and now allowed (decay into on-shell $W^{\pm}$ and into top quarks). The large uncertainty is due to propagation of the error of $\cos\theta$. With these values we could reproduce the total widths of the NW and to the LW within the errors by adding a large decay width of h_1 into $h_2 h_2$. [17]

A more detailed analysis is needed to accept or reject the validity of the model. If we focus now on the quantity $\sigma(pp \to h_2)\text{BR}(h_2 \to \gamma\gamma)$ we find values of $\mathcal{O}(10^{-13})$ fb - $\mathcal{O}(10^{-14})$ fb, which cannot reproduce the experimental data.

6.1.2 Light scenario

Remember from Section 4.2.2 how the best-fit value for the angle was $\cos\theta = 0.99 \pm 0.01$, exactly as in the heavy scenario with a redefinition of the angle and with the difference that now the decay of the other Higgs-like particle cannot have contributions from the decay to lighter scalars, i.e. $h_2 \to h_1 h_1$, so the analysis for this scenario will be identical as the previous one with $\Gamma_{h_1 \to h_2 h_2} = 0$, and the observed excess cannot be reproduced.

6.2 Diphoton excess in the A2HDM

In this section we will analyze the possibility of the observed resonance to be one of the scalars of the A2HDM, in the limit in which CP is conserved. As we have seen in Section 5.5.3 the χ^2 seem to exclude the possibility of the 125 GeV observed Higgs being the CP-odd Higgs, so in this section we will not treat this unlikely possibility and we will assume the 125 GeV Higgs is a CP-even Higgs (sections 5.5.1 and 5.5.2) with the previous results of the fit. Inside this scenario three different possibilities can be studied. First of all, the resonance could be due to a heavy CP-even scalar, H, whose diphoton rate can be enhanced by a charged-particle loop of $H^{\pm}$ as we will see in Section 6.2.1. Secondly, there exist the more unlikely possibility that the responsible particle of the excess may be the odd Higgs, A. In this context it is more difficult to reproduce the experimental data, since the loop of $H^{\pm}$ is not present in the decay of A into photons (Section 6.2.2). Finally, if the masses of H and A are degenerated or quasi-degenerated, the resonance could be a consequence of the decays of the two particles together, as will be analyzed in Section 6.2.3. We will see how the excess cannot be reproduced at the same time as all the couplings remain perturbative.

6.2.1 Heavy even Higgs

From the fit results of Eq. (168) and the relations of Eq. (154) values for $\mathcal{R}_{21} = -\sin\tilde{\alpha}$ and y_f^H can be obtained:

$$\sin\tilde{\alpha} = 0.20 \pm 0.20\,, \quad y_u^H = -0.20 \pm 0.37\,, \quad |y_d^H| = 0.88 \pm 0.44\,, \quad |y_l^H| = 0.25 \pm 0.77\,. \tag{174}$$

In this case the cross sections and decay widths are very similar to the case of the light scalar, with the difference that now the channels $H \to XX$ with $XX = VV, ZZ, t\bar{t}, hh$ are kinematically allowed. Further, the decay width of $H \to \gamma\gamma$ may be enhanced by the charged scalar loop, $H^{\pm}$. At this point, and taking the parameters of (174), only $\Gamma_{H \to H^+ H^-}$ $\Big($or what is the same, $\mathcal{C}^H_{H^{\pm}} = \mathcal{C}^H_{H^{\pm}}(\lambda_{HH^+H^-}, M_{H^{\pm}})\Big)$ and $\Gamma_{H \to hh}$ are undetermined.

[17] Which should be checked that is perturbative.

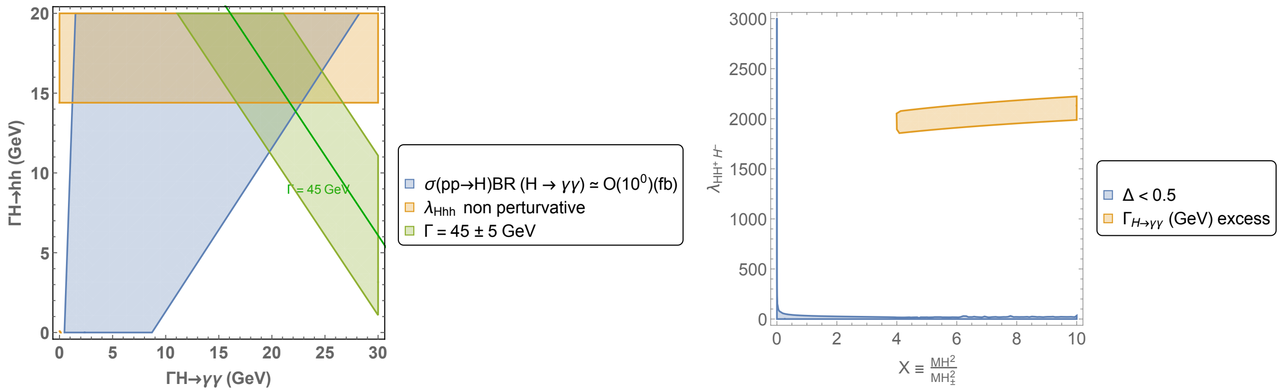

Figure 18: **Left:** In blue values of $\Gamma_{H\to H^+H^-}$ and $\Gamma_{H\to hh}$ for which the order of magnitude for $\sigma_{pp\to S}BR_{S\to\gamma\gamma}$ is reproduced. In green the region for which the total width reproduces the LW hypothesis and in orange it is shown the region in which λ_{Hhh} is not perturbative. **Right:** Region that reproduces the desired signal (orange) and region where the coupling $\lambda_{HH^+H^-}$ remains perturbative (blue).

Without setting these parameters, and taking into account the other decays the total decay width is

$$\Gamma_H = \Gamma_{H\to\gamma\gamma} + \Gamma_{H\to hh} + 8.92^{+16.10}_{-8.92}\ \text{GeV}\,, \tag{175}$$

It can be checked that there is no overlap between the values reproducing the NW fit ($\Gamma = 0.1$ GeV) and the order of magnitude of $\sigma_{pp\to S}BR_{S\to\gamma\gamma}$ desired.

For the LW fit, with suitable values of $\Gamma_{H\to H^+H^-}$ and $\Gamma_{H\to hh}$ the experimental results of $\sigma_{pp\to S}\text{BR}_{S\to\gamma\gamma}$ can be reproduced. In Fig. 18 possible values of $\Gamma_{H\to H^+H^-}$ and $\Gamma_{H\to hh}$ giving the excess in the diphoton signal are shown. Since the data are still limited and the values of ATLAS and CMS differ we analyze the region in which $\sigma_{pp\to S}BR_{S\to\gamma\gamma} \approx \mathcal{O}(10^1)$ fb (blue). The green area shows the region for which the total width is $\Gamma = 45 \pm 5$ GeV, i.e, the LW hypothesis, with an uncertainty of the 10%. In orange the non-perturbative region for λ_{Hhh} is shown, according to the discussion of Appendix C. The values $\Gamma_{H\to H^+H^-}$ and $\Gamma_{H\to hh}$ that would meet our requirements will be contained in the overlap of the blue region with the green one, and not overlapping with the non-perturbative region of λ_{Hhh} indicated in orange. The perturbativity of $\Gamma_{H\to H^+H^-}$ still has to be checked.

The allowed range of $\Gamma_{H\to H^+H^-}$ can be translated in possible values of $\lambda_{HH^+H^-}$ and $M_{H_\pm}$. As it can be seen in the right panel of Fig. 18, the values of $\lambda_{HH^+H^-}$ that will reproduce the excess are very large ($\lambda_{HH^+H^-} > 1500$) and comparing this with the perturbative region, it can be seen that the regions do not overlap, which means if the diphoton excess is reproduced with these values of $\lambda_{HH^+H^-}$ and $M_{H_\pm}$ it would not be perturbative.

The values that better approach to the experimental data remaining perturbative correspond to $\lambda_{HH^+H^-} \approx 20$ and $X \equiv \frac{M_H^2}{M_{H\pm}^2} \approx 9.9$, giving a $\sigma_{pp\to S}BR_{S\to\gamma\gamma}$ of the order $\mathcal{O}(10^{-3})$ fb. If we relax the perturbativity constraints into $\Delta < 1$ (see Appendix C for details), we get $\lambda_{HH^+H^-} \approx 30$ and $X \approx 9.9$, a slight improvement, doubling the value $\sigma_{pp\to S}BR_{S\to\gamma\gamma}$, but still very far from the order of magnitude needed.

6.2.2 Heavy odd Higgs

In this section we will explore the possibility of the resonance observed to be the heavy odd scalar of the A2HDM, A. There are two main characteristics of the odd boson that seem to discard this possibility. First of all, since $W^\pm$ and Z bosons do not couple to A at tree level, the dominant contribution for $\Gamma_{A\to VV}$ will start at one loop (Appendix B), consequently being very suppressed. Further, as we have previously seen, in the CP-conserving limit A does not couple to the charged bosons, $H^\pm$, so in this case any loop mediated via H^+H^- particles cannot enhance the photon signal.

To see that in detail, let's consider the values or the coupling obtained through the relations of Eq. (154):

$$\mathcal{R}_{31} = 0\,, \qquad y_u^A = (0.02 \pm 0.27)i\,, \qquad y_d^A = (0.69 \pm 0.91)i\,, \qquad y_l^A = (0.01 \pm 3.57)i\,. \tag{176}$$

The first we note is the large uncertainties in the parameters, that will later be translated into large uncertainties in our results. The total decay width obtained, using Eq. (176) is

$$\Gamma_A = 0.02^{+7.17}_{-0.02}\,\text{GeV}\,, \tag{177}$$

automatically ruling out the LW fit, and if we look at $\sigma(pp \to A)BR(A \to \gamma\gamma)$ we obtain an order of magnitude of $\mathcal{O}(10^{-8})$ fb - $\mathcal{O}(10^{-9})$ fb, very far from the experimental value.

6.2.3 Heavy and odd (degenerate mass)

Lastly, we will briefly analyze the unlikely possibility of the masses of H and A being degenerate. If the two bosons have such close masses that the observed resonance is due to their combination, the observed signal and the calculated decay width will be the sum of both contributions, i.e, $\Gamma = \Gamma_H + \Gamma_A$. In principle it may look that it is a simple way to increase the diphoton signal. However, since we have seen in 6.2.2 that the contribution of the odd particle is negligible in front of the even scalar, our analysis will be reduced into the one of Section 6.2.1.

7 Conclusions

In this work the best theory physicist have to describe fundamental particles and their interactions with high precision, the SM, has been introduced, showing how dynamical forces arise from the gauge principle together with the symmetries of the model. Phenomenology of strong, electromagnetic and weak interactions has also been studied. As an attempt to solve the fact that masses are forbidden by gauge symmetry, the Higgs boson and the process of SSB have been introduced, showing how, with this new ingredient fermions and weak bosons acquire mass.

Even though the great success of the SM, which has passed very precise test of the 0.1 % to 1% some features of nature, such as the sources of CP-violation, related to the matter-antimatter asymmetry in the Universe or the experimental evidence of dark matter, are not well-explained with only the ingredients of the SM. This, together with the freedom to extend the scalar sector of the SM with certain conditions is the main motivation for the two models studied here: the Higgs singlet extension and the A2HDM.

The Higgs singlet extension is the simplest modification of the scalar sector. Basically, it consists in adding an extra real bosonic singlet, invariant under all the quantum numbers of the SM gauge group. The addition of such new particle increases the number of parameters from 2 to 7 and the new singlet is mixed with the SM Higgs. Due to this mixing, a rotation matrix needs to be introduced to diagonalize the states and this, together with the fact that the singlet is invariant under $SU(2)_L \otimes U(1)_Y$ transformations introduces a modification in the Yukawa Lagrangian, so that the two bosons (in the mass eigenstates basis) are coupled to fermions with a reduced factor of $\sin\theta$ / $\cos\theta$. A new interesting ingredient of this model is the possibility of having a dark matter (DM) candidate in the decoupling limit $\cos\theta = 1$. Given that the new scalar couple feebly to ordinary fermions via the Higgs boson it is a good candidate for cold DM (particles that interact with themselves with considerable σ but weakly with ordinary matter) [27] .

The other extension studied, the A2HDM, includes more interesting new ingredients. In this model, an identical doublet as the SM's Higgs doublet (the same quantum numbers) is added. As a result, three scalars, S_i, two CP-even and one CP-odd appear after the SSB. Since the interaction states are not mass eigenstates an orthogonal rotation needs to be introduced to relate the fields S_i with the mass eigenstates $\varphi_i^0 = h, H, A$. In general, these bosons will be mixed, while in the CP-conserving limit, where the imaginary parts of the couplings are set to be zero, the mixing between even and odd bosons disappear.

Since the new doublet has the same quantum numbers as the SM one, more terms can be added to the Yukawa Lagrangian. The alignment in flavour space of the Yukawa couplings is an essential property of the model, introduced to avoid FCNC, tightly constrained experimentally. The alignment has interesting consequences, as explained in Section 5. The phenomenology of this model, is richer than for the previous extension, since the coupling between the odd scalar and the fermions is not present in the SM. The existence of a charged particle, $H^{\pm}$, is also a novelty of the A2HDM which has interesting consequences as the addition of new diagrams contributing to the decay of Higgs scalars into photons, or in the meson mixing, not studied here.

For both models, an statistical analysis has been performed by minimizing the χ^2 function containing the experimental Higgs strengths of the data and the theoretical ones predicted by the models. Depending on the value of χ^2 / d.o.f. the goodness of the fit made these possibilities more or less unlikely, finding as the most viable possibility the A2HDM with the observed Higgs a CP-even boson.

ATLAS and CMS have recently presented preliminary results of Run 2 of LHC, showing an excess of the diphoton signal corresponding to an invariant mass around 750 GeV. Such excess has been studied in the context of these two extensions. Adding a real singlet, as in the Higgs singlet extension, these excess cannot be reproduced, as it is explained in Section 6.1. The A2HDM contains more new ingredients with respect to the SM, among them the previously mentioned charged particle $H^{\pm}$ which can enhance the diphoton signal. To reproduce the experimental signal the coupling constant of such particle, $\lambda_{HH^+H^-}$, will not be perturbative applying the criterion of Appendix C. To reproduce the experimental signal a non-perturbative cubic coupling $\lambda_{HH^+H^-}$ would be needed. LHC data showing the excess are still preliminary and the excess may be due just to statistical fluctuations. To confirm or reject that, new data will be needed.

Other interesting ingredients of the A2HDM not studied here are the DM implications. The Inert A2HDM (IDM) (discrete $\mathcal{Z}_2$ symmetry in the Higgs basis and therefore $\varsigma_f = 0$) is of special interest for studying these DM implications and the relic abundance can be obtained. [18] In this model the lightest scalar particle, h, is the SM Higgs boson, while the two remaining scalars are DM candidates. Constraints and numerical analysis for this model have been studied as in [28].

In the future, and thanks to the abilities acquired while doing this work more detailed analysis of the A2HDM could be done by studying the theoretical and experimental constraints of the model and exploring other interesting consequences as the just mentioned DM ingredients and the sources of CP violation.

A Phenomenological analysis with the χ^2 function

In this section we will explain the procedure used to perform a global fit in the models studied. Such procedure is based on the minimization of the χ^2 function, and uses as input the experimental data of the Higgs searches and the SM predictions.

The experimental data on the Higgs searches are usually given in terms of the so called signal strengths, the measured cross sections in units of the SM expectations. The relevant processes to consider at the LHC for a SM Higgs are gluon fusion ($gg \to H$), vector boson fusion ($qq' \to qq'VV \to qq'H$), associated production with a vector boson ($q\bar{q'} \to WH/ZH$) and associated production with a $t\bar{t}$ pair ($q\bar{q}/gg \to t\bar{t}H$).

[18] However, for the IDM to be a correct model for baryogenesis extra ingredients need to be added, because CP violation occurs only in the CKM matrix as in the SM.

Channel	$\hat{\mu}_k$
$b\bar{b}$	1.09 ± 0.91
$b\bar{b}V$	0.65 ± 0.3
$WWjj$	1.38 ± 0.39
WW	1.44 ± 0.36
$ZZjj$	0.48 ± 1.16
ZZ	1.00 ± 0.22
$\tau^+\tau^-$	1.10 ± 0.60
$\tau^+\tau^- V$	1.12 ± 0.36
$\gamma\gamma$	1.19 ± 0.27
$\gamma\gamma jj$	1.05 ± 0.43

Table 2: Higgs signal strengths for the channels considered. Averages from ATLAS and CMS at $s = \sqrt{7}$ and $s = \sqrt{8}$ TeV respectively.

To perform the fit let's consider the following signal strengths:

$$\mu_{bb}^{\varphi_i^0} \equiv \frac{\sigma(pp \to \varphi_i^0)Br(\varphi_i^0 \to b\bar{b})}{\sigma(pp \to H)_{SM} Br(H \to b\bar{b})_{SM}}, \qquad \mu_{\gamma\gamma}^{\varphi_i^0} \equiv \frac{\sigma(pp \to \varphi_i^0)Br(\varphi_i^0 \to \gamma\gamma)}{\sigma(pp \to H)_{SM} Br(H \to \gamma\gamma)_{SM}}, \tag{178}$$
$$\mu_{\tau\tau}^{\varphi_i^0} \equiv \frac{\sigma(pp \to \varphi_i^0)Br(\varphi_i^0 \to \tau\tau)}{\sigma(pp \to H)_{SM} Br(H \to \tau\tau)_{SM}}, \qquad \mu_{\gamma\gamma jj}^{\varphi_i^0} \equiv \frac{\sigma(pp \to jj\varphi_i^0)Br(\varphi_i^0 \to \gamma\gamma)}{\sigma(pp \to jjH)_{SM} Br(H \to \gamma\gamma)_{SM}},$$
$$\mu_{bbV}^{\varphi_i^0} \equiv \frac{\sigma(pp \to V\varphi_i^0)Br(\varphi_i^0 \to b\bar{b})}{\sigma(pp \to VH)_{SM} Br(H \to b\bar{b})_{SM}}, \qquad \mu_{VV}^{\varphi_i^0} \equiv \frac{\sigma(pp \to \varphi_i^0)Br(\varphi_i^0 \to VV)}{\sigma(pp \to H)_{SM} Br(H \to VV)_{SM}},$$
$$\mu_{\tau\tau V}^{\varphi_i^0} \equiv \frac{\sigma(pp \to V\varphi_i^0)Br(\varphi_i^0 \to \tau\tau)}{\sigma(pp \to VH)_{SM} Br(H \to \tau\tau)_{SM}}, \qquad \mu_{VVjj}^{\varphi_i^0} \equiv \frac{\sigma(pp \to jj\varphi_i^0)Br(\varphi_i^0 \to VV)}{\sigma(pp \to jjH)_{SM} Br(H \to VV)_{SM}},$$

where $V = W, Z$ and j stands for jet.

The experimental values for the signal strengths combining the last results of ATLAS and CMS are given in Table 2. [29]

For a given choice of a neutral scalar field, the χ^2 function is defined as usual,

$$\chi^2(\varphi_i^0) = \sum_k \frac{\left(\mu_k^{\varphi_i^0} - \mu_k\right)^2}{\sigma_k^2}, \tag{179}$$

where k runs over all the significant decay/production channels and μ_k and σ_k are the measured Higgs signal strengths and their uncertainties, as it can be seen in Table 2.

The parameters of our model are contained in $\mu_k^{\varphi_i^0}$. The procedure to find the best value for these parameters consists in the minimization of the χ^2 function of Eq.(179), and the uncertainties are given by their CL, obtained by increasing the function χ^2 a certain quantity depending on d.o.f. and in the desired CL. A table with the values of $\Delta\chi^2$ for the differents CL and d.o.f. can be seen in [30]. The goodness of the fit also depends on the number of d.o.f. and this is the reason why we have always mentioned $\chi^2/$ d.o.f. and not just χ^2.

Finally, in the cases in which the errors are asymmetric but close, and to use the standard error propagation the following formula to symmetrize the errors is used:

$$\delta X = \sqrt{\frac{(\delta X_+)^2 + (\delta X_-)^2}{2}}, \tag{180}$$

being $\delta X_\pm$ the one-sided errors.

B Phenomenology of the A2HDM

In this appendix, detailed calculations of the processes involving the Higgs-like scalars are given, both for the CP-even scalars (H and h) and for the CP-odd scalar (A), being processes involving this last particle different than the SM ones as we have seen in the theoretical discussion of the model in Section 5.

Since the length available is limited only some of the processes are included in this appendix. Other processes as $pp \to jj\varphi_i^0$ have also been calculated.

B.1 Decay channels

B.1.1 Decay into a fermion pair

The decay of a Higgs-like scalar, φ_i^0 into a pair of fermions can be seen in Fig. 12 (left) with the convention of p_1 as the incoming momentum of φ_i^0 and p_2 and p_3 the momenta the outgoing fermion pair.

In the case of the CP-even scalar, the amplitude matrix reads:

$$\mathcal{M} = \bar{u}_2\Big(- \frac{m_f y_f^{\varphi_i^0}}{v}\Big) v_3 \,, \tag{181}$$

being u_i and v_j the spinors of the particle with momentum p_i. The squared amplitude matrix is:

$$\begin{aligned}\sum_{r_2,r_3} |\mathcal{M}|^2 \equiv |\overline{\mathcal{M}}|^2 &= \frac{|y_f^{\varphi_i^0}|^2 m_f^2}{v^2} \,\mathrm{Tr}\left[(\not{p}_2 + m_f)\,(\not{p}_3 - m_f)\right] = 4\frac{|y_f^{\varphi_i^0}|^2 m_f^2}{v^2}(p_2\cdot p_3 - m_f^2) \\ &= 2\frac{|y_f^{\varphi_i^0}|^2 m_f^2}{v^2}(M^2_{\varphi_i^0} - 4m_f^2) = 2\frac{|y_f^{\varphi_i^0}|^2 m_f^2}{v^2} M^2_{\varphi_i^0}\big(1 - \frac{4m_f^2}{M^2_{\varphi_i^0}}\big) = 2\frac{|y_f^{\varphi_i^0}|^2 m_f^2}{v^2} M^2_{\varphi_i^0}\beta_f^2 \,,\end{aligned} \tag{182}$$

where we have used conservation of the 4-momentum, $p_1^2 = m^2_{\varphi_i^0} = (p_2 + p_3)^2 = 2m_f^2 + 2p_2 p_3$ and the β_f function is defined as:

$$\beta_X \equiv \sqrt{1 - \frac{4m_X^2}{M^2_{\varphi_i^0}}} \,. \tag{183}$$

To find the decay width we integrate over the phase space:

$$\Gamma^{even}(\varphi_i^0 \to f\bar{f}) = \frac{1}{2M_{\varphi_i^0}} \int dQ_2 |\overline{\mathcal{M}}|^2 = N_C \frac{|y_f^{\varphi_i^0}|^2 m_f^2}{8\pi v^2} M_{\varphi_i^0}\beta_f^3 \,, \tag{184}$$

N_C is the number of colours, $N_C = 3$ for quarks and $N_C = 1$ for leptons.

For the odd scalar the results are slightly different. The matrix element takes the form:

$$\mathcal{M} = \bar{u}_2\Big(- \frac{m_f y_f^{\varphi_i^0}\gamma_5}{v}\Big) v_3 \,. \tag{185}$$

The square matrix element:

$$\begin{aligned}|\overline{\mathcal{M}}|^2 &= \frac{|y_f^{\varphi_i^0}|^2 m_f^2}{v^2} \,\mathrm{Tr}\left[(\not{p}_2 + m_f)\,\gamma_5(\not{p}_3 - m_f)\gamma_5\right] = 4\frac{|y_f^{\varphi_i^0}|^2 m_f^2}{v^2}(p_2\cdot p_3 + m_f^2) \\ &= 2M^2_{\varphi_i^0}\frac{|y_f^{\varphi_i^0}|^2 m_f^2}{v^2} \,.\end{aligned} \tag{186}$$

And the decay width:

$$\Gamma^{odd}(\varphi_i^0 \to f\bar{f}) = \frac{1}{2M_{\varphi_i^0}} \int dQ_2 |\overline{\mathcal{M}}|^2 = N_C \frac{|y_f^{\varphi_i^0}|^2 m_f^2}{8\pi v^2} M_{\varphi_i^0}\beta_f \,. \tag{187}$$

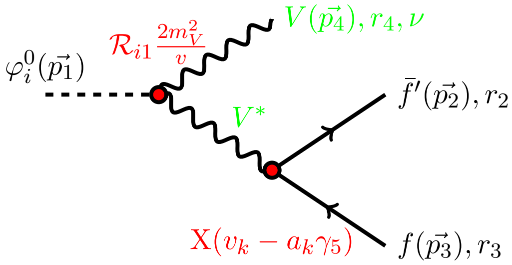

Figure 19: Decay of the scalar φ_i^0 into a virtual and a on-shell boson.

In the decays into quarks, quantum corrections are an important contribution, and must be added. They are included by evaluating the running quark masses on the Higgs scale and introducing the correction as given in [31] (with n_f the number of flavours):

$$\tilde{R}(\alpha_s, n_f) = 1+5.66667\Big(\frac{\alpha_s(M_{\varphi_i^0})}{\pi}\Big)+(35.94-1.359n_f)\Big(\frac{\alpha_s(M_{\varphi_i^0})}{\pi}\Big)^2+(164.1-25.77n_f+0.259n_f^2)\Big(\frac{\alpha_s(M_{\varphi_i^0})}{\pi}\Big)^3 . \tag{188}$$

B.1.2 Decay into weak bosons

The decay of a Higgs-like scalar into weak bosons would be on-shell, if the mass of the scalar is above the kinematic threshold or into a virtual and on-shell boson if the mass is below the threshold.[19] For the on-shell decay we would have a process as shown in Fig. 12 (right), independently of the CP-parity of the boson, with the following amplitude:

$$\mathcal{M} = \frac{2M_v^2}{v}\mathcal{R}_{i1}\varepsilon_{\mu,2}\varepsilon_3^\mu , \tag{189}$$

and

$$\sum_{r_2,r_3}|\mathcal{M}|^2 = \frac{4M_v^4}{v^2}\mathcal{R}_{i1}^2\Big(-g_{\mu\nu}+\frac{p_{2\mu}p_{2\nu}}{M_v^2}\Big)\Big(-g^{\mu\nu}+\frac{p_3^\mu p_3^\nu}{M_v^2}\Big) = \frac{4M_v^4}{v^2}\mathcal{R}_{i1}^2\Big(3+\frac{1}{4}\frac{M_{\varphi_i^0}^4}{M_v^4}-\frac{M_{\varphi_i^0}^2}{M_v^2}\Big) . \tag{190}$$

Using the result of the phase space of Section B.1.1 the decay width takes the form:

$$\Gamma(\varphi_i^0 \to W^+W^-) = \frac{1}{4\pi}\frac{M_W^4}{v^2 M_{\varphi_i^0}}\mathcal{R}_{i1}^2\beta_W\Big(3+\frac{1}{4}\frac{M_{\varphi_i^0}^4}{M_W^4}-\frac{M_{\varphi_i^0}^2}{M_W^2}\Big) , \tag{191}$$

$$\Gamma(\varphi_i^0 \to ZZ) = \frac{1}{8\pi}\frac{M_Z^4}{v^2 M_{\varphi_i^0}}\mathcal{R}_{i1}^2\beta_Z\Big(3+\frac{1}{4}\frac{M_{\varphi_i^0}^4}{M_Z^4}-\frac{M_{\varphi_i^0}^2}{M_Z^2}\Big) , \tag{192}$$

with β_X as defined in Eq.(183). The relative $\frac{1}{2}$ factor between the two decays is due to the fact that ZZ are identical particles.

If the mass of φ_i^0 is below the kinematic threshold, it would decay into a virtual and an on-shell bosons, as it can be seen in Fig. 19. Here, we consider together the cases of the decay into ZZ^* and into WW^*. For the first one we would have $\mathrm{X} = \frac{e}{2c_{\mathrm{W}}s_{\mathrm{W}}}$ and $v_k = v_f$, $a_k = a_f$, while for the decay into WW^*, $X = \frac{g}{2\sqrt{2}}V_{ud}$ and $(v_k - a_k\gamma_5) = (1-\gamma_5)$. Regarding to the final states, they will be f and $\bar{f}$ for Z as final state and f_u, $\bar{f}_d$ for W as final state. We will do it assuming massless fermions.

For the matrix element, in the unitary gauge, with $q = p_1 - p_4 = p_2 + p_3$:

$$\mathcal{M} = -\frac{2M_v^2}{v}X\mathcal{R}_{i1}\bar{v}_2\gamma_\mu(v_k - a_k\gamma_5)u_3\frac{g_{\mu\nu}-\frac{q_\mu q_\nu}{M_v^2}}{q^2-M_v^2}\varepsilon_{\nu 4} . \tag{193}$$

[19] Since $M_W = 80.4$ GeV and $M_Z = 91.2$ GeV, for the scalar to decay on-shell into W bosons, $M_{\varphi_i^0} > 160.8$ GeV, and to decay both into W and Z, $M_{\varphi_i^0} > 182.4$ GeV,

The square matrix element involves a trace, Tr:

$$|\overline{\mathcal{M}}|^2 = \frac{4M_v^4}{v^2}\mathcal{R}_{i1}^2 (Tr)_{\mu\mu'}(P)^{\mu\mu'}\frac{1}{(q^2-M_v^2)^2}\,, \tag{194}$$

with

$$\begin{aligned}(Tr)_{\mu\mu'} &= \mathrm{Tr}\big[\not{p}_2\gamma_\mu(v_k-a_k\gamma_5)\not{p}_3(v_k+a_k\gamma_5)\gamma'_\mu\big] \\ &= 4(a_k^2+v_k^2)[p_{2\mu}p_{3\mu'}+p_{2\mu'}p_{3\mu}-g_{\mu\mu'}(p_2p_3)] - 8a_kv_ki\epsilon_{\mu'\mu\alpha\beta}p_2^\alpha p_3^\beta\,.\end{aligned} \tag{195}$$

After some algebra

$$\begin{aligned}(P)^{\mu\mu'} &= -\Big(g^{\mu\nu}-\frac{q^\mu q^\nu}{M_v^2}\Big)\Big(g^{\mu'\nu'}-\frac{q^{\mu'}q^{\nu'}}{M_v^2}\Big)\Big(g_{\nu\nu'}-\frac{p_{4\nu}p_{4\nu'}}{M_v^2}\Big) \\ &= -\left[g^{\mu\mu'}-2\frac{q^\mu q^{\mu'}}{M_v^2}+q^2\frac{q^\mu q^{\mu'}}{M_v^2}-\frac{p_4^\mu p_4^{\mu'}}{M_v^2}+2(p_4\cdot q)\frac{q^\mu p_4^{\mu'}}{M_v^4}-(p_4\cdot q)^2\frac{q^\mu q^{\mu'}}{M_v^6}\right]\,.\end{aligned} \tag{196}$$

To write it in a more compact way let's consider:

$$s_{ij} = (p_i+p_j)^2\,, \tag{197}$$

with that

$$(Tr)_{\mu\mu'}(P)^{\mu\mu'} = -4M_{\varphi_i^0}^2 + 4s_{24} + 8s_{34} + \frac{4s_{24}}{M_v^2}(s_{24}+s_{34}-M_{\varphi_i^0}^2)\,. \tag{198}$$

And the corresponding phase space integral, with $x = \frac{M_v^2}{M_{\varphi_i^0}^2}$ and $s_{min}=0$, $s_{max} = M_{\varphi_i^0}^2 + M_v^2 - s_{24} - \frac{M_{\varphi_i^0}^2 m_v^2}{s_{24}}$,

$$\int_{s_{min}}^{s_{max}} dQ_3 \frac{(Tr)_{\mu\mu'}(P)^{\mu\mu'}}{(q^2-M_v^2)^2} = \frac{S(x)}{768\pi^3 x}\,, \tag{199}$$

with

$$S(x) = 47x^2-60x+15-\frac{2}{x}-3(4x^2-6x+1)\ln(x) - \frac{6(20x^2-8x+1)}{(4x-1)^{\frac{1}{2}}}\arccos\big(\frac{3x-1}{2x^{3/2}}\big)\,. \tag{200}$$

The decay width for Wf_uf_d reads:

$$\begin{aligned}\Gamma(\varphi_i^0\to Wf_u\bar{f}_d) &= \frac{g^2}{2v^2}\frac{M_W^2\mathcal{R}_{i1}^2}{M_{\varphi_i^0}^2}N_C\sum_{u,d}|V_{u,d}|^2\int_{s_{min}}^{s_{max}}dQ_3\frac{(Tr)_{\mu\mu'}(P)^{\mu\mu'}}{(q^2-M_W^2)^2} \\ &= \frac{g^2}{v^2}\frac{3M_W^2}{256\pi^3}M_{\varphi_i^0}S(x)\,.\end{aligned} \tag{201}$$

For the decay into a $Zf\bar{f}$:

$$\Gamma(\varphi_i^0\to Zf\bar{f}) = \frac{e^2\mathcal{R}_{i1}^2}{c_{\mathrm{w}}^2 s_{\mathrm{w}}^2}\frac{M_z^2}{1536v^2\pi^3}M_{\varphi_i^0}S(x)\sum_f(a_f^2+v_f^2)\,, \tag{202}$$

and performing the sum over v_f and a_f (which previously was just 2),

$$\begin{aligned}\sum_f(v_f^2+a_f^2) &= N_C\left[\sum_{i=u,c}(a_i^2+v_i^2)+\sum_{i=d,s,b}(a_i^2+v_i^2)\right]+3\left[(a_l^2+v_l^2)+(a_\nu^2+v_\nu^2)\right] \\ &= 18\Big(\frac{7}{12}-\frac{10}{9}\sin^2\theta_{\mathrm{w}}+\frac{40}{27}\sin^4\theta_{\mathrm{w}}\Big)\equiv 18R(\theta_{\mathrm{w}})\,.\end{aligned} \tag{203}$$

So, the decay width takes the form

$$\Gamma(\varphi_i^0\to Zf\bar{f}) = \frac{e^2\mathcal{R}_{i1}^2}{c_{\mathrm{w}}^2 s_{\mathrm{w}}^2}\frac{3M_z^2}{256v^2\pi^3}M_{\varphi_i^0}S(x)R(\theta_{\mathrm{w}})\,. \tag{204}$$

B.1.3 Decay $\varphi_i^0 \to \gamma\gamma$ through a H^+H^- loop

In this section we will calculate the contribution of the $H^\pm$ loop to the decay $\varphi_i^0 \to \gamma\gamma$ as it is seen in Fig. 13. Of course, these two diagrams are completed with a third, identical to the first with the crossing of the photon external lines and the full decay width of $\varphi_i^0 \to \gamma\gamma$ is completed with diagrams containing quarks and $W^\pm$ loops.

For the first diagram we have:

$$\begin{aligned}\mathcal{M}_1 = v\lambda\varepsilon_2^\mu\varepsilon_3^\nu \int \frac{d^dk}{(2\pi)^d}(2k_\mu + p_{2\mu})(-2k_\nu + p_{3\nu}) \\ \frac{1}{k^2 - M_{H^\pm}^2}\frac{1}{(k-p_3)^2 - M_{H^\pm}^2}\frac{1}{(k+p_2)^2 - M_{H^\pm}^2} \\ = v\lambda e^2\varepsilon_2^\mu\varepsilon_3^\nu \int \frac{d^dk}{(2\pi)^d}\frac{4k_\mu k_\nu}{(k^2 - M_{H^\pm}^2)((k-p_3)^2 - M_{H^\pm}^2)((k+p_2)^2 - M_{H^\pm}^2)}\,,\end{aligned} \tag{205}$$

where some terms have vanished due to transversality, $\varepsilon_i^\alpha p_{i\alpha} = 0$.

Now we can use Feynman parametrization:

$$\frac{1}{ABC} = \int_0^1 dx \int_0^1 dy \int_0^1 dz\delta(x+y+z-1)\frac{2}{[Ax+By+Cz]^3}\,. \tag{206}$$

Using that:

$$\frac{1}{(k^2 - M_{H^\pm}^2)\Big((k-p_3)^2 - M_{H^\pm}^2\Big)\Big((k+p_2)^2 - M_{H^\pm}^2\Big)} = \int_0^1 dx \int_0^{1-x} dy \frac{1}{(k'^2 - a^2)^3}\,, \tag{207}$$

with $k' = k + p_2y - p_3z$ and $a^2 = M_{H^\pm}^2 - 2p_2p_3yz$. Performing the change in the variable of integration $dk \to dk'$ we get:

$$\mathcal{M}_1 = 4v\lambda e^2\varepsilon_2^\mu\varepsilon_3^\nu \int_0^1 dx \int_0^{1-x} dy \int \frac{d^dk'}{(2\pi)^2}\frac{2(k'_\mu k'_\nu - p_{3\mu}p_{2\nu}yz)}{(k'^2 - a^2)^3}\,. \tag{208}$$

We have two different integrals that can be calculated using the following expression with $d = 4+2\epsilon$:

$$\begin{aligned}\mathcal{J}(d,\alpha,\beta,a^2) = \int \frac{d^dk'}{(2\pi)^d}\frac{(k'^2)^\alpha}{(k'^2 - a^2 + i\epsilon)^\beta} \\ = \frac{i}{(4\pi)^{d/2}}(a^2)^{d/2}(-a^2)^{\alpha-\beta}\frac{\Gamma(\beta-\alpha-d/2)\Gamma(\alpha+d/2)}{\Gamma(\beta)\Gamma(d/2)}\,.\end{aligned} \tag{209}$$

The first one:

$$I_{\mu\nu} = \int \frac{d^dk'}{(2\pi)^2}\frac{2k'_\mu k'_\nu}{(k'^2 - a^2)^3} = 2\frac{g_{\mu\nu}}{d}\mathcal{J}(d,1,3,a^2)\,. \tag{210}$$

This integral have a divergent part and another finite:

$$I_{\mu\nu} = \frac{i}{(4\pi)^2}(a^2)^\epsilon\frac{\Gamma(-\epsilon)(\epsilon+2)}{2} = \frac{i}{(4\pi)^2}\Big(-\frac{1}{\hat\epsilon} - \frac{1}{2} - \ln a^2\Big)\,, \tag{211}$$

with $\frac{1}{\hat\epsilon} = \frac{1}{\epsilon} + \gamma_E$. For the second one we find:

$$I_1 = \int \frac{d^dk'}{(2\pi)^2}\frac{1}{(k'^2 - a^2)^3} = \mathcal{J}(d,0,3,a^2) = -\frac{i}{(4\pi)^{d/2}}(a^2)^{d/2}(-a^2)^{-3}\frac{\Gamma(-1-\epsilon)}{\Gamma(3)}(a^2)^{\epsilon-1} = -\frac{i}{(4\pi)^2}\Big(\frac{1}{2a^2}\Big)\,.$$

Combining these, for $\mathcal{M}_1$ we find:

$$\mathcal{M}_1 = 4v\lambda e^2\varepsilon_2^\mu\varepsilon_3^\nu\frac{i}{(4\pi)^2}\int_0^1 dx \int_0^{1-x} dy \left\{\frac{g_{\mu\nu}}{4}(-\frac{1}{\hat\epsilon} - \frac{1}{2} - \ln a^2) - p_{3\mu}p_{2\nu}xy\frac{1}{a^2}\right\}\,. \tag{212}$$

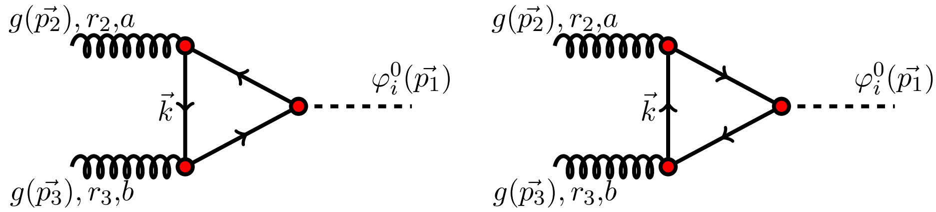

Figure 20: Production of φ_i^0 through gluon fusion.

It is easy to see that the diagram whose only difference with $\mathcal{M}_1$ is the external photon lines (let's call it $\mathcal{M}_2$), gives exactly the same contribution,

$$\mathcal{M}_1 = \mathcal{M}_2\,. \tag{213}$$

The other diagram can be seen in the right of Fig. 13 and has as matrix element:

$$\mathcal{M}_3 = -v\lambda e^2 g_{\mu\nu}\varepsilon_2^\mu\varepsilon_3^\nu \int \frac{d^dk}{(2\pi)^2}\frac{1}{k^2-M_{H^\pm}^2}\frac{1}{(k-p_1)^2-M_{H^\pm}^2}\,. \tag{214}$$

Using the following Feynman parametrization

$$\frac{1}{AB} = \int_0^1 dx\int_0^1 dy\delta(x+y-1)\frac{1}{[Ax+By]^2}\,, \tag{215}$$

$\mathcal{M}_3$ takes the form:

$$\mathcal{M}_3 = -v\lambda e^2 \varepsilon_2^\mu\varepsilon_{3\mu}\int_0^1 dy\int\frac{d^dk'}{(2\pi)^2}\frac{1}{(k'^2-b^2)^2}\,, \tag{216}$$

with the change $k' = k - p_1 y$ and $b^2 = M_{H^\pm}^2 y(y-1) + M_{H^\pm}^2$. As before, we have an integral we will calculate using (209):

$$\begin{aligned} I_2 &= \int\frac{d^dk'}{(2\pi)^2}\frac{1}{(k'^2-b^2)^2} = \mathcal{J}(d,0,2,b^2) \\ &= \frac{i}{(4\pi)^{d/2}}(b^2)^\epsilon\Gamma(-\epsilon) = \frac{i}{(4\pi)^2}(-\frac{1}{\hat{\epsilon}}-\ln b^2)\,. \end{aligned} \tag{217}$$

And

$$\mathcal{M}_3 = -v\lambda e^2\varepsilon_2^\mu\varepsilon_{3\mu}\frac{i}{(4\pi)^2}\int_0^1 dy\Big(-\frac{1}{\hat{\epsilon}}-\ln b^2\Big)\,. \tag{218}$$

Adding the contribution of (212), (213) and (218) we see the divergent terms cancel and the finite parts can be integrated numerically, and squared give us:

$$|\overline{\mathcal{M}}|^2 = \frac{M_{\varphi_i^0}^4}{2v^2}\frac{\alpha}{\pi^2}\Big|\frac{v^2}{2M_{H_\pm}^2}\lambda_{\varphi_i^0 H^+H^-}\mathcal{A}(x_{H_\pm})\Big|^2\,, \tag{219}$$

with $\mathcal{A}(x)$ as defined in (164) and $x_{H_\pm} = \frac{4M_{H_\pm}^2}{M_{\varphi_i^0}^2}$.

B.2 Production channels

B.2.1 Gluon-gluon fusion

The production of the scalar, φ_i^0 through gluon fusion can be seen in Fig. 20

Due to the $\varphi_i^0 q\bar{q}$ vertex, the contribution of the even and the odd scalars will be different. We will start with the CP-even scalar, for which $\mathcal{M}_1$, corresponding to the left diagram, takes the form:

$$\begin{aligned}\mathcal{M}_1 &= -ig_s^2 \frac{m_q}{v} \varepsilon^a_{\mu,r_2} \varepsilon^b_{\mu,r_3} \left(\frac{\lambda_a}{2}\right)_{\delta\gamma} \left(\frac{\lambda_b}{2}\right)_{\delta'\gamma'} \delta_{\delta\delta'} \delta_{\gamma'\sigma} \delta_{\sigma\gamma} \\ \int \frac{d^d k}{(2\pi)^d} & \frac{\mathrm{Tr}\left[\gamma^\mu (\not{k} + \not{p}_2 + m_q)(\not{k} - \not{p}_3 + m_q)\gamma^\nu (\not{k} + m_q)\right]}{D_1 \cdot D_2 \cdot D_3} \\ &= -ig_s^2 \frac{m_q}{v} \varepsilon^a_{\mu,r_2} \varepsilon^b_{\mu,r_3} \left(\frac{\lambda_a}{2}\right)_{\delta\sigma} \left(\frac{\lambda_b}{2}\right)_{\delta\sigma} I^{\mu\nu}\end{aligned} \tag{220}$$

with

$$\begin{aligned} D_1 &= k^2 - m_q^2 \\ D_2 &= (k + p_2)^2 - m_q^2 \\ D_3 &= (k - p_3)^2 - m_q^2 \end{aligned} \tag{221}$$

The colour trace is:

$$\left(\frac{\lambda_a}{2}\right)_{\delta\sigma} \left(\frac{\lambda_b}{2}\right)_{\sigma\delta} = \mathrm{Tr}\left(\frac{\lambda_a}{2}\frac{\lambda_b}{2}\right) = \frac{1}{2}\delta_{ab} \,. \tag{222}$$

And the spinor trace:

$$\begin{aligned} &\mathrm{Tr}\left[\gamma^\mu (\not{k} + \not{p}_2 + m_q)(\not{k} - \not{p}_3 + m_q)\gamma^\nu (\not{k} + m_q)\right] \\ &= 4m_q(-k^2 g_{\mu\nu} + m_q^2 g^{\mu\nu} - g^{\mu\nu}(p_2 \cdot p_3) + 4k^\mu k^\nu + 2k^\nu p^\mu - 2k^\mu p_3^\nu + p_2^\nu p_3^\mu - p_2^\mu p_3^\nu) \equiv 4m_q N^{\mu\nu} \,. \end{aligned} \tag{223}$$

As we haven seen in Eq. (206) performing a Feynman parametrization, we get

$$\frac{1}{D_1 \cdot D_2 \cdot D_3} = \int_0^1 dy \int_0^{1-y} dz \frac{2}{[(k + p_2 y - p_3 z)^2 - a^2]^3} \,. \tag{224}$$

With the transformation $k' = k + p_2 y - p_3 z$ and with $a^2 = m_q^2 - 2(p_2 \cdot p_3) yz$ and eliminating the vanishing terms proportional to and k and k^α the tensor reads $N^{\mu\nu}$,

$$\begin{aligned} N^{\mu\nu} \to N'^{\mu\nu} &= 4k'^\mu k'^\nu - g^{\mu\nu} k^2 + p_3^\mu p_2^\nu (1 - 4yz) \\ &+ p_2^\mu p_3^\nu (-1 - 4yz + 2y + 2z) + p_3^\mu p_3^\nu (4z^2 - 2z) \\ &+ p_2^\mu p_2^\nu (4y^2 - 2y) + g^{\mu\nu}(m_q^2 - p_2 \cdot p_3 + 2p_2 \cdot p_3 yz) \,. \end{aligned} \tag{225}$$

The integral $I^{\mu\nu}$ can be separated in two pieces:

$$\begin{aligned} I^{\mu\nu} &= \int_0^1 dy \int_0^{1-y} dz \int \frac{d^d k'}{(2\pi)^d} \frac{8m_q N'^{\mu\nu}}{(k'^2 - a^2)^3} \\ &= 8m_q \int_0^1 dy \int_0^{1-y} dz \left\{ I_1^{\mu\nu} + (p_3^\mu p_2^\nu (1 - 4yz) + g^{\mu\nu}(m_q^2 - p_2 \cdot p_3 + 2p_2 \cdot p_3 yz)) I_2 \right\} \,, \end{aligned} \tag{226}$$

where we have eliminated the vanishing terms due to transversality. The integrals can be calculated:

$$I_1^{\mu\nu} = \int \frac{d^d k'}{(2\pi)^d} \frac{4k'^\mu k'^\nu - g^{\mu\nu} k'^2}{(k'^2 - a^2)^3} = \left(\frac{4}{d} - 1\right) g^{\mu\nu} \mathcal{J}(d, 1, 3, a^2) = \frac{i}{32\pi^2} g^{\mu\nu} \,, \tag{227}$$

$$I_2 = \mathcal{J}(d, 0, 3, a^2) = \frac{-i}{32\pi^2} \frac{1}{a^2} \,. \tag{228}$$

And defining

$$\int_0^1 dy \int_0^{1-y} dz \frac{1}{-a^2}(1 - 4yz) \equiv C \tag{229}$$

we find

$$I^{\mu\nu} = \frac{8im}{32\pi^2} C [p_3^\mu p_2^\nu - g^{\mu\nu} p_2 \cdot p_3] \,. \tag{230}$$

As we can see from Fig. 20 the second diagram will give us the same contribution so $|\overline{\mathcal{M}}|^2 = 4|\overline{\mathcal{M}}_1|^2$ and

$$|\overline{\mathcal{M}}|^2 = \frac{1}{64} g_s^2 \frac{\alpha^2}{v^2\pi^2} m_q^2 |\mathcal{F}(x_q)|^2 \,, \tag{231}$$

with $\mathcal{F}$ coming from the integral in (229) and defined in Eq. (164).

For the odd scalar, we will have the same diagrams, but now the transition amplitude will be different

$$\begin{aligned} \mathcal{M}_1 &= -i g_s^2 \frac{m_q}{2v} \varepsilon^a_{\mu,r_2} \varepsilon^b_{\mu,r_3} \delta_{ab} \\ \int \frac{d^d k}{(2\pi)^d} & \frac{\mathrm{Tr}\left[\gamma^\mu (\not{k} + \not{p}_2 + m_q)\gamma_5(\not{k} - \not{p}_3 + m_q)\gamma^\nu(\not{k} + m_q)\right]}{D_1 \cdot D_2 \cdot D_3} \\ &= i g_s^2 \frac{m_q}{2v} \varepsilon^a_{\mu,r_2} \varepsilon^b_{\mu,r_3} \delta_{ab} I^{\mu\nu} \,. \end{aligned} \tag{232}$$

The only difference with respect to (220) is the trace, which now takes the form:

$$\mathrm{Tr}\left[\gamma^\mu (\not{k} + \not{p}_2 + m_q)\gamma_5(\not{k} - \not{p}_3 + m_q)\gamma^\nu(\not{k} + m_q)\right] = 4 i m_q p_{2\alpha} p_{3\beta} \epsilon^{\alpha\beta\mu\nu} \equiv A^{\mu\nu} \,, \tag{233}$$

with the same Feynman parametrization as in the case of the even scalar:

$$I^{\mu\nu} = \int_0^1 dy \int_0^{1-y} dz \frac{2A^{\mu\nu}}{(k^2 - a^2)^3} \,. \tag{234}$$

The only integral has already been calculated in Eq. (228). With that $I^{\mu\nu}$ takes the form:

$$I^{\mu\nu} = \frac{m_q}{4\pi^2} p_{2\alpha} p_{3\beta} \epsilon^{\alpha\beta\mu\nu} \int_0^1 dy \int_0^{1-y} dz \frac{1}{a^2} = \frac{m_q}{4\pi^2} p_{2\alpha} p_{3\beta} \epsilon^{\alpha\beta\mu\nu} I_3 \,. \tag{235}$$

As before, adding the other identical diagram and performing the integral of Eq. (235) we get:

$$|\overline{\mathcal{M}}|^2 = \frac{g_s^2 \alpha^2 m_q^2}{64 v^2 \pi^2} |\mathcal{K}(x_q)|^2 \,, \tag{236}$$

with the loop function, $\mathcal{K}(x)$ defined in (164).

In order to calculate the cross section, the one-particle phase space is needed:

$$\int dQ_1 \equiv \int \frac{d^3 p}{2E} \delta^{(4)}(P_i - P_f) = 2\pi \delta(s - M_{\varphi^2}) \,, \tag{237}$$

and

$$\hat{\sigma}(gg \to \varphi_i^0) = \frac{\pi}{256 M^2_{\varphi_i^0}} \delta(s - M_{\varphi^2}) |\overline{\mathcal{M}}|^2 \,. \tag{238}$$

Finally, we have to integrate using the parton distribution functions (PDF) that can be found in `http://projects.hepforge.org/mstwpdf/`. To do this, we consider two protons carrying momenta P_1 and P_2 (with $p_{gi} = x_i P_i$) and x_i the momentum fractions ($0 \leq x_i \leq 1$). The PDF functions have the form $g(x, \mu)$, with μ being the scale .

$$\begin{aligned} s &= (p_{g_1} + p_{g_2})^2 = (x_1 P_1 + x_2 P_2)^2 = x_1 x_2 S \,, \\ \delta(s - M^2_{\varphi_i^0}) &= \delta(x_1 x_2 S - M^2_{\varphi_i^0}) = \frac{1}{x_1 S} \delta(x_2 - \frac{M^2_{\varphi_i^0}}{x_1 S}) \,. \end{aligned} \tag{239}$$

The cross section

$$\begin{aligned} \sigma(gg \to \varphi_i^0) &= \int dx_1 \int dx_2 g(x_1, \mu) g(x_2, \mu) \hat{\sigma}(gg \to \varphi_i^0) \\ &= \frac{\pi}{256 M^2_{\varphi_i^0} S} \int_{\frac{M^2_{\varphi_i^0}}{S}}^1 |\mathcal{M}|^2 \frac{dx_1}{x_1} g(x_1, \mu) g\Big(\frac{M^2_{\varphi_i^0}}{S x_1}, \mu\Big) \,. \end{aligned} \tag{240}$$

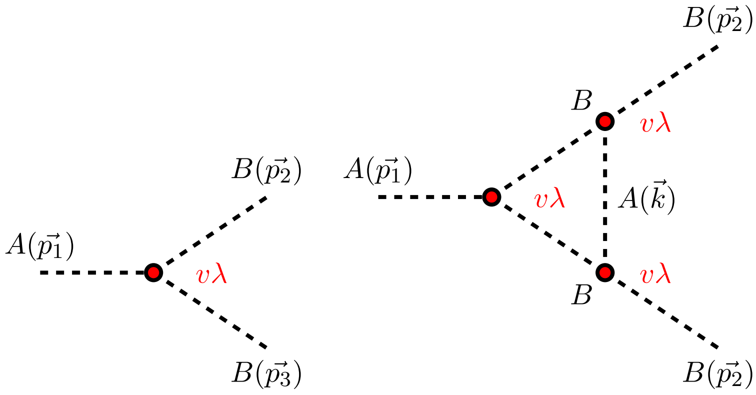

Figure 21: Diagram of the tree-level vertex (left) and one-loop correction (right) of Hhh and $\varphi_i^0 H^+ H^-$ (A = φ_i^0, H and B = $H^\pm, h$).

C Perturbativity constraints

In previous sections we have mentioned the perturbative constraints of processes like $H \to hh$ or $\varphi_i^0 \to \gamma\gamma$. In this section the criterion used will be explained. Unlike in other references where perturbativity constraints are taken from requiring the couplings to be smaller than a certain value, i.e. 8π [15], here we consider the effective coupling one-loop correction to be smaller than the tree-level vertex (at most a 50%).

We will do that for the two processes previously mentioned, since they share the same structure (with $A = \varphi_i^0$, H and $B = H^\pm$, h). The tree-level vertex and its one-loop correction are given in Fig. 21.

The tree level amplitude is just:

$$\mathcal{M}_{TL} = iv\lambda\,. \tag{241}$$

The one-loop contribution is finite:

$$\begin{aligned}\mathcal{M}_{1L} = (iv\lambda)^3 \int \frac{d^dk}{(2\pi)^d} \frac{i}{k^2 - m_A^2} \frac{i}{(k+p_2)^2 - m_B^2} \frac{i}{(k+p_1)^2 - m_B^2} \\ = \frac{i\lambda^3 v^3}{(4\pi)^2 m_B^2} \mathcal{Z}\Big(\frac{m_A^2}{m_B^2}\Big)\,,\end{aligned} \tag{242}$$

with

$$\mathcal{Z}(X) = \int_0^1 dy \int_0^{1-y} dz[(y+z)^2 + X(1-y-z-yz)]^{-1}\,. \tag{243}$$

And we have used Feynman parametrization and performed the integral using (209).

Once the tree level and one-loop amplitude have been calculated, it can be seen that the effective vertex at one-loop takes the form:

$$iv\lambda_{eff} = iv\lambda + \frac{iv\lambda^3 v^3}{16\pi^2 m_B^2} \mathcal{Z}\Big(\frac{m_A^2}{m_B^2}\Big) \to \lambda_{eff} = \Big[1 + \frac{v^2\lambda^2}{16\pi^2 m_B^2}\Big(\frac{m_A^2}{m_B^2}\Big)\Big] \equiv \lambda(1+\Delta)\,, \tag{244}$$

with

$$\Delta = \frac{v^2\lambda^2}{16\pi^2 m_B^2} \mathcal{Z}\Big(\frac{m_A^2}{m_B^2}\Big)\,.$$

And we say the vertex λ is perturbative if $\Delta < 0.5$.

References

[1] A. Pich, arXiv:1201.0537 [hep-ph].

[2] D. Griffiths, "Introduction to elementary particles" Wiley, 1987

[3] S. F. Novaes, In *Sao Paulo 1999, Particles and fields* 5-102 [hep-ph/0001283].

[4] F. Halzen and A. D. Martin, "Quarks and leptons" Wiley, 1985

[5] A. Pich, In *Sorrento 1994, High energy physics* 157-207 [hep-ph/9505231].

[6] A. Pich, hep-ph/0001118.

[7] A. Deur, S. J. Brodsky and G. F. de Teramond, arXiv:1604.08082 [hep-ph].

[8] P. W. Higgs, Phys. Rev. Lett. **13** (1964) 508. doi:10.1103/PhysRevLett.13.508

[9] F. Englert and R. Brout, Phys. Rev. Lett. **13** (1964) 321. doi:10.1103/PhysRevLett.13.321

[10] G. S. Guralnik, C. R. Hagen and T. W. B. Kibble, Phys. Rev. Lett. **13** (1964) 585. doi:10.1103/PhysRevLett.13.585

[11] T. W. B. Kibble, Phys. Rev. **155** (1967) 1554. doi:10.1103/PhysRev.155.1554

[12] J. Goldstone, A. Salam and S. Weinberg, Phys. Rev. **127** (1962) 965. doi:10.1103/PhysRev.127.965

[13] R. A. Diaz and R. Martinez, Rev. Mex. Fis. **47** (2001) 489 [hep-ph/0302058].

[14] A. Pich, Acta Phys. Polon. B **47** (2016) 151 doi:10.5506/APhysPolB.47.151 [arXiv:1512.08749 [hep-ph]].

[15] T. Robens and T. Stefaniak, Eur. Phys. J. C **75** (2015) 104 doi:10.1140/epjc/s10052-015-3323-y [arXiv:1501.02234 [hep-ph]].

[16] G. C. Branco, P. M. Ferreira, L. Lavoura, M. N. Rebelo, M. Sher and J. P. Silva, Phys. Rept. **516** (2012) 1 doi:10.1016/j.physrep.2012.02.002 [arXiv:1106.0034 [hep-ph]].

[17] A. Pich and P. Tuzon, Phys. Rev. D **80** (2009) 091702 doi:10.1103/PhysRevD.80.091702 [arXiv:0908.1554 [hep-ph]].

[18] T. P. Cheng and M. Sher, Phys. Rev. D **35** (1987) 3484. doi:10.1103/PhysRevD.35.3484

[19] A. Celis, V. Ilisie and A. Pich, JHEP **1307** (2013) 053 doi:10.1007/JHEP07(2013)053 [arXiv:1302.4022 [hep-ph]].

[20] K. Cheung, J. S. Lee and P. Y. Tseng, JHEP **1305** (2013) 134 doi:10.1007/JHEP05(2013)134 [arXiv:1302.3794 [hep-ph]].

[21] G. Abbiendi *et al.* [ALEPH and DELPHI and L3 and OPAL and LEP Collaborations], Eur. Phys. J. C **73** (2013) 2463 doi:10.1140/epjc/s10052-013-2463-1 [arXiv:1301.6065 [hep-ex]].

[22] The ATLAS collaboration, ATLAS-CONF-2015-081.

[23] CMS Collaboration [CMS Collaboration], CMS-PAS-EXO-15-004.

[24] V. Khachatryan *et al.* [CMS Collaboration], Phys. Lett. B **750** (2015) 494 doi:10.1016/j.physletb.2015.09.062 [arXiv:1506.02301 [hep-ex]].

[25] S. Di Chiara, L. Marzola and M. Raidal, Phys. Rev. D **93** (2016) no.9, 095018 doi:10.1103/PhysRevD.93.095018 [arXiv:1512.04939 [hep-ph]].

[26] J. M. No, arXiv:1605.05900 [hep-ph].

[27] D. E. Holz and A. Zee, Phys. Lett. B **517** (2001) 239 doi:10.1016/S0370-2693(01)01033-4 [hep-ph/0105284].

[28] M. Krawczyk, N. Darvishi and D. Sokolowska, Acta Phys. Polon. B **47** (2016) 183 doi:10.5506/APhysPolB.47.183 [arXiv:1512.06437 [hep-ph]].

[29] The ATLAS and CMS Collaborations, ATLAS-CONF-2015-044.

[30] J. Zuñiga. Lectures on Experimental Techniques of Nuclear and Particle Physics. Year 2015-2016. Master in Advance Physics, Universitat de València

[31] P. A. Baikov, K. G. Chetyrkin and J. H. Kuhn, Phys. Rev. Lett. **96** (2006) 012003 doi:10.1103/PhysRevLett.96.012003 [hep-ph/0511063].